POLITECNICO DI TORINO
Repository ISTITUZIONALE

From by-products to biomaterials for active wound dressings

Original
From by-products to biomaterials for active wound dressings / Ferraris, S., Alfieri, M.L., Najmi, Z., Vineis, C., Savino, E., Varesano, A., Spriano, S., Rimondini, L., Cochis, A.. - In: MATERIALS TODAY COMMUNICATIONS. - ISSN 2352-4928. - 54:(2026), pp. 1-17. [10.1016/j.mtcomm.2026.115661]

Availability:
This version is available at: 11583/3012650 since: 2026-07-03T07:04:44Z

Publisher:
Elsevier

Published
DOI:10.1016/j.mtcomm.2026.115661

Terms of use:

This article is made available under terms and conditions as specified in the corresponding bibliographic description in the repository

Publisher copyright

(Article begins on next page)

19 November 2026

Materials Today Communications 54 (2026) 115661

Contents lists available at ScienceDirect

Materials Today Communications

journal homepage: www.elsevier.com/locate/mtcomm

From by-products to biomaterials for active wound dressings

Sara Ferraris [a,1], Maria Laura Alfieri [b,1], Ziba Najmi [c], Claudia Vineis [d,*], Erica Savino [d], Alessio Varesano [d], Silvia Spriano [a], Lia Rimondini [c], Andrea Cochis [c]

[a] Department of Applied Science and Technology, Politecnico di Torino, Italy
[b] Department of Chemical Sciences, Università di Napoli Federico II, Napoli, Italy
[c] Department of Health Sciences, Center for Translational Research on Autoimmune and Allergic Diseases CAAD, Università del Piemonte Orientale UPO, Novara, Italy
[d] CNR-STIIMA (National Research Council of Italy - Institute of Intelligent Industrial Technologies and Systems for Advanced Manufacturing), Biella, Italy

ARTICLE INFO

Keywords:
By-products
Keratin
Polyphenols
Nanofibers
Biomaterials
Antibacterial
Antioxidant

ABSTRACT

Innovative multifunctional biomaterials should properly improve the performance of wound dressings by promoting tissue healing while preventing side events such as bacterial infection and excessive inflammation. Moreover, the sustainable design of new materials can result in environmentally friendly and cost-effective solutions. However, very few of the available dressings satisfy all of these characteristics, and none are derived from a renewable source. Herein, bioactive compounds obtained from industrial by-products were applied to develop active wound dressings that combine antioxidant and antibacterial activities, combining multifunctionality and a sustainable approach. Accordingly, the fabric was obtained by electrospun keratin nanofibers (NF) obtained from discarded wool, while bioactivity was introduced through NF functionalization with polyphenols-rich extracts from pomegranate and grape by-products. Keratin fabrics were checked by Scanning Electron Microscopy (SEM) and Fourier Transform Infrared Spectroscopy (FT-IR) confirming the stability of the NF random structure, while extracts were analyzed by UV-Vis and HPLC demonstrating the presence of bioactive phenols such as punicalagin, ellagic acid and catechins. NF functionalization was confirmed by Zeta potential and Folin&Ciocalteu, as well as phenols antioxidant activity was verified by 2,2-diphenyl-1-picrylhydrazyl (DPPH), ferric reducing/antioxidant power (FRAP) and cupric reducing antioxidant capacity (CUPRAC) assays. Afterward, a preliminary biological characterization revealed that the dressings were cytocompatible towards human fibroblasts (>90% viability), as well as the NF functionalization reported a significant ($p < 0.05$) scavenger activity preventing the intracellular internalization of toxic ROS active species (>90% reduction). Finally, pomegranate functionalization significantly ($p < 0.05$) prevented surface contamination by *Staphylococcus epidermidis* of > 95% compared to non-functionalized NF, as well it successfully reduced the infection *in situ* after being released from the dressing.

1. Introduction

Skin serves as the first line of defense between the human body and the external environment and, consequently, is particularly vulnerable to damage. Skin wounds can be categorized into acute wounds, such as mechanical and chemical injuries, and chronic wounds, including burns, infections, and diabetes-related wounds [1]. Effective wound management is crucial for preventing post-surgical complications, thus decreasing hospitalization time and costs. Dressing materials are classified into two categories based on their interaction with the wound: passive dressings, which simply protect the wound, and active dressings, which support healing by creating a pro-regenerative environment. More specifically, an ideal active dressing should provide support against mechanical stress, absorb exudate, reduce bleeding, prevent infections, and mitigate inflammation [2]. Although a wide range of wound dressings is currently available (e.g., gauze, cotton wool and plasters), none of them simultaneously meet all these requirements, and their high costs make them inaccessible to most of the population in most cases [3]. A possible solution to lower the costs of active dressings could be to use industrial by-products as the base material with a green and sustainable approach, but to date none of the dressings available come from or use recycled materials [3]. Recently, nanofiber (NF)

* Correspondence to: CNR-STIIMA, Biella, Italy.
E-mail address: claudia.vineis@cnr.it (C. Vineis).
[1] Co-shared authorship

https://doi.org/10.1016/j.mtcomm.2026.115661
Received 16 March 2026; Received in revised form 12 June 2026; Accepted 2 July 2026
Available online 2 July 2026
2352-4928/© 2026 The Authors. Published by Elsevier Ltd. This is an open access article under the CC BY license (http://creativecommons.org/licenses/by/4.0/).

membranes have gained significant attention in biomedical applications, being produced from a wide variety of bio-based and synthetic polymers. Because of their characteristics, NF membranes find applications in various fields (such as air filtration and waste treatment), including biomedical uses like wound healing, cellularized scaffolds, and drug delivery [4]. One of the most applied methods for obtaining NFs is represented by electrospinning, which can be applied to a wide variety of polymers, including protein-based biopolymers. A particularly promising biopolymer for the development of NF is keratin, a fibrous protein found in feathers, hair, wool, horns, and nails of mammals, birds, and reptiles, which represents an essential source of renewable raw materials [5]. Moreover, keratin is one of the main components of by-products from the textile and slaughterhouse industries, thus representing an attractive candidate for a second use in high-value products, while it is considered an environmental pollutant and a threat to the ecosystem by now. This protein has a high cysteine content (7–13%) compared to other structural proteins, which allows the formation of inter- and intra-chain disulfide bonds, providing increased stability and reduced solubility in most solvents. In fact, to obtain water-soluble keratin extracts, the disulfide bonds must be broken through chemical or physical methods [6]. The electrospinning of regenerated keratin extracted from waste wool can provide an eco-friendly, inexpensive, and biocompatible scaffold that supports cell adhesion, proliferation, and migration, thereby promoting tissue repair during wound healing [6]. However, keratin has limited antibacterial and anti-inflammatory capabilities on its own, therefore the bioactive properties required to meet the clinical needs must be provided by further functionalization. In this frame, polyphenols are natural substances, mainly present in fruits, vegetables and plants, well known for their health benefits such as antioxidant, antibacterial, vasculo-protective, bone-stimulating, anticancer, and immunomodulating properties [7–9]. Due to their proven bioactivity, these molecules have been widely studied in traditional medicine, phytotherapy and nutraceutics [10,11]. An increasing interest has been evidenced in recent years in the combination of polyphenols with biomaterials to improve their bioavailability and apply their biological activities for local treatment of different diseases, as well as in tissue regeneration, antibacterial and anti-inflammatory implantable materials [12,13]. Polyphenols have already been reported in the literature as active ingredients in biomaterials intended for wound dressing [14–16] because they can regulate the healing process even in hard-to-heal wounds (e.g. diabetic, chronic) due to their ability to support antioxidant defense, reducing oxidative stress, modulate the inflammatory response, reducing the infection rate and enhance tissue regeneration through improved angiogenesis and collagen synthesis [17]. Despite these promising premises, a very limited literature reported about keratin and polyphenols application for wound-healing applications [18–20]: among these, some papers combine keratin and polyphenols with the use of additional materials, such as cellulose hydrogel, polyurethane matrix, silk or graphene oxide. In the majority of the examples, keratin and polyphenols are combined in the form of nanocapsules for local delivery [6], but not as the functionalization of keratin fibers with active molecules. Most importantly, none of them employs natural polyphenols from by-products, but mostly commercially available processed or synthetic products, thus failing to consider a sustainable approach. On the contrary, agri-food by-products could represent a sustainable and abundant source of phenolic compounds endowed with potent antioxidant, anti-inflammatory and/or antimicrobial properties [21,22]. Since the disposal of these by-products entails cost for processors and harms the environment, their recovery represents a valuable and sustainable opportunity. In particular, the attention has been focused here on grape pomace and pomegranate peel seeds, abundantly produced in Europe and rich in phenolic compounds endowed with strong antioxidant, anti-inflammatory, and antibacterial properties [23,24]. Based on these premises, in this work, randomly oriented NFs of keratin from discarded wool and natural polyphenols extracted from grape and pomegranate were directly combined for the first time in this work to obtain sustainable, cytocompatible dressings with antioxidant and antibacterial properties able to meet clinical needs. To the best of our knowledge, this represent a first attempt to obtain multifunctional antibacterial and anti-inflammatory active dressings by using only materials from by-products and green synthesis, thus matching clinical requirements and sustainability. The obtained dressings were characterized for their physicochemical properties and antioxidant activity to assess the functionalization of keratin with polyphenols and their activity, followed by a preliminary biological evaluation to confirm cytocompatibility, antioxidant and antibacterial properties.

2. Materials and methods

2.1. Materials

Urea, sodium metabisulfate ($Na_2S_2O_5$), polyethylene oxide (PEO, average Mw 400 kDa), 2,2-diphenyl−1-picrylhydrazyl (DPPH), iron (III) chloride ($FeCl_3$), 2,4,6-tris(2-pirydyl)-s-triazine (TPTZ), Folin-Ciocalteu reagent, vanillin, neocuproine, copper chloride ($CuCl_2$), copper nitrate, potassium chloride, phosphate buffered saline (PBS, tablet), sodium carbonate, gallic acid and hydrogen peroxide (30% w/v) were purchased from Sigma-Aldrich. Grape pomace was kindly provided by a winery, whereas pomegranate was purchased at a local supermarket.

2.2. Methods

UV−Vis spectra were recorded on a Jasco V−730 or UV 2600 Shimadzu spectrophotometers.

HPLC analyses were performed on an Agilent 1100 binary pump instrument equipped with an SPD−10AV VP UV-Visible detector set at 254 nm. The chromatographic separation was achieved using an octadecylsilane-coated column, 250 mm × 4.6 mm, 5 μm particle size (Phenomenex Sphereclone ODS) at 0.7 mL/min using binary gradient elution conditions as follows: 0.1% formic acid (solvent A)/methanol (solvent B) at 5% B in the first 10 min and from 5% to 80%, from 10 to 47.5 min.

LC-UV-MS analysis were performed on an Agilent ESI-TOF 1260/6230DA instrument coupled with a UV-Vis detector set at 254 nm, in negative ion mode in the following conditions: nebulizer pressure 35 psig; drying gas (nitrogen) 10 L/min, 325 °C; capillary voltage 3500 V; fragmentor voltage 175 V. An Eclipse Plus C18 column, 150 × 4.6 mm, 5 μm, at a flow rate of 0.4 mL/min was used, with 0.1% formic acid (eluant A)–methanol (eluant B) under the gradient condition described above.

2.2.1. Keratin extraction

A wool sample, provided by the International Wool Textile Organisation (IWTO), was cleaned using Soxhlet extraction with petroleum ether to eliminate fatty substances, washed with distilled water, and conditioned at 20 °C and 65% relative humidity for 24 h. Then, 5 g of cleaned and conditioned fibers were cut into pieces of a few millimeters and treated with 100 mL of an aqueous solution containing urea (8 M), $Na_2S_2O_5$ (0.5 M) and sodium dodecyl sulfate (SDS, 0.05 M), adjusted to pH 6.5 with NaOH 5 N, under shaking for 2 h at 65°C. Using a peristaltic pumping system, the resulting solution was separated from the solid fraction through a series of filtration steps with progressively thinner meshes up to a 5-micron pore-sized membrane. Following filtration, the solution underwent dialysis for three days against distilled water using cellulose tubes with a molecular weight cut-off of 12–14 kDa to eliminate all the chemical residues. The water was replaced four times per day. After completing dialysis, the solution was freeze-dried to obtain pure keratin powder with a molecular weight of 30–45 kDa. The final expected yield of keratin extraction by sulfitolysis is 38 ± 5%, as previously reported [25].

Table 1
Operational parameters for producing the NF-membranes.

Solvent	Total Polymer Conc. (%w/v)	Polymer Blend (% w/v)	Flow Rate (mL min−1)	Tip-Collector Distance (cm)	Voltage (kV)	Needle i.d. (mm)	Air temperature (C°)	Relative humidity (%)
Water (mQ)	7	70/30 KS/PEO	0.01	22	25	0.2	21–24	30–35

2.2.2. Keratin nanofiber (NF) production

The selected solution blend composition had a total polymer concentration of 7% wt, with a keratin/polyethylene oxide ratio of 70:30, representing the optimum balance between high keratin content and desirable physical properties of the solution, in agreement with previous works [5,26,27]. The NF membranes were fabricated using a single-jet electrospinning setup which included a flat plate collector, a KDS 200 high-precision syringe pump (KD Scientific Inc., USA), a 27-gauge stainless-steel needle (0.41 mm outer diameter, 0.21 mm inner diameter), and an SL50 high-voltage generator (Spellman, UK). The electrospinning process parameters (voltage, flow rate, polymer concentration, tip-to-collector distance, air temperature, and humidity) were varied to determine the optimal conditions for producing homogeneous NFs with minimal bead formation. The optimized operational parameters for making the keratin/PEO NF membrane are detailed in Table 1. The NF were deposited on various substrates, such as commercial cotton gauze and glass for 2 h of electrospinning in each batch. Part of the substrates were treated with an air plasma (10 min, 100 W, TUCANO2, Gambetti Kenologia Srl) before keratin deposition to improve the adhesion, as previously observed by the authors [28].

All samples were post-treated to prevent water-solubilization of proteins by heating them in an oven for 2 h at 180°C. This process promotes the cross-linking of keratin chains, enhancing their stability while simultaneously sterilizing the samples. The water-soluble PEO used as an electrospinning processing aid was removed by soaking the fibers in water at mild stirring conditions and temperature for 24 h.

3. Physicochemical characterization

3.1. NFs characterization

The morphology of NFs was observed using an EVO 10 Scanning Electron Microscope (SEM, Carl Zeiss Microscopy GmbH) at an acceleration voltage of 20 kV and a working distance of about 30 mm. The samples were sputter-coated with a 20 nm-thick gold layer in a rarefied argon atmosphere (20 Pa) using a Quorum Q150RES Plus sputter coater with a current of 20 mA for 120 s. Fourier Transform Infrared Spectroscopy (FT-IR) spectra were recorded by a Thermo Nicolet iN10 spectrometer equipped with an iZ10 module, a Smart Endurance accessory (with a diamond crystal ZnSe focusing element) in attenuated total reflection within a range of 4000–650 cm^{-1} with 50 scans and a band resolution of 4 cm^{-1}.

3.2. Preparation of polyphenol extracts

In the case of pomegranate, the waste (peel and seeds) was separated from the edible part, rapidly cut into small pieces and freeze-dried. After that, the lyophilized material was shredded using a blender. The resulting pomegranate-waste powder (1 g) and grape pomace (1 g) were extracted with water (10 mL, 100 mg/mL solid-to-liquid ratio) under stirring (350 rpm) for 1 h at room temperature. The mixtures were then centrifuged (7000 rpm) for 15 min and the supernatants (PE and GPE for pomegranate wastes and grape pomace, respectively) were recovered, analysed by UV-Vis and LC-UV-MS and stored at −25 °C. The solid residues were instead lyophilized to evaluate the extracted ponderal yield by difference (*ca.* 55% w/w for both extracts).

3.3. Surface functionalization

For the functionalization, stabilized (thermal treatment 2 h@180°C) keratin NFs (on gauze or on glass) were soaked in aqueous solutions of PE or GPE (10 mg/mL) for 3 h at 37°C. In this case, no 24 h soaking in water of the fibers was performed, PEO solubilization was performed directly in the functionalization media. The procedure simultaneously allows the grafting of polyphenol and the removal of PEO. After that, the samples were gently washed in ultrapure water and air-dried under a laminar flow cabinet. In order to maximize electrostatic attraction between polyphenols and keratin NFs, two different functionalization conditions were considered: acidic and neutral. In the first case, polyphenols (both GE and GPE) were diluted in ultrapure water at a concentration of 10 mg/mL: the pH of the solution was around 3.7, and the NF functionalized in these conditions will be named ker _PE_ac and ker _GPE_ac from now on. For the neutral functionalization, polyphenols were diluted in TRIS/HCl buffer solution (pH 7.4) and added with copper nitrate $Cu(NO_3)_2$. The LD50 of copper ions (14.6 mg/mL, [29]) was used as the limit concentration in the buffer solution, considering that the amount of Cu^{2+} ions loaded on the fibers will be significantly lower. Copper ions have been introduced as possible linkers for polyphenols grafting, as previously reported by the authors [30] and discussed in the following: NF functionalized in these conditions will be named ker _PE_neu and ker _GPE_neu from now on. For biological tests, functionalization was performed on sterile thermally-treated samples under clean conditions: stem-sterilized water and glassware, 0.2 μm filtration of polyphenolic solutions, and preparation under a sterile laminar flow hood.

3.3.1. Zeta potential titration curves

Zeta potential measurements were performed on a 0.5 mg/mL solution of PE and GPE in 0.001 M KCl as electrolyte, by means of electrophoretic measurements (Litesizer 500 Anton Paar equipped with omega cuvette). The pH of the solution was varied in the acidic and basic range by manual addition of 0.05 M HCl and 0.05 M NaOH, respectively. 3 measurements were performed for each pH point. Zeta potential titration curves on solid samples (ker, ker_PE_ac, ker_PE_neu, ker_GPE_ac and ker_GPE_neu) were performed by means of an electrokinetic analyser (SurPASS, Anton Paar) equipped with an adjustable gap cell, using 0.001 M KCl as electrolyte and varying the pH through the acidic and basic range with the automatic titration unit of the system (0.05 M HCl added for the acidic range and 0.05 M NaOH added for the basic one). Keratin NFs deposited on glass substrates were used for these tests. The same set of samples was used for acidic and basic titrations, and the acidic one was done first.

3.3.2. Release test

The polyphenols released in physiological and pro-inflammatory conditions were monitored up to 14 days. PBS at physiological pH (7.4) was used to simulate a physiological environment, while PBS added with H_2O_2 (0.05 M final concentration in PBS) and HCl (to reach pH of 4.5) was considered to mimic pro-inflammatory conditions [31]. Samples were soaked in 15 mL of the solution at 37 °C up to 14 days. The solution was changed at 1 and 7 days, and samples were collected after 14 days. The total amount of polyphenols in the solutions and on solid samples (at the beginning and at the end of the test) was quantified by means of the total phenolic content assay (Folin&Ciocalteu test) as described in the following 2.5.3 chapter.

3.3.3. Total phenolic content (TPC) assay

Total polyphenols on keratin NF have been quantified by the Folin&Ciocalteu test adapted to solid samples (TPC) [32]. In brief, each sample (1 ×1 cm keratin NFs deposited on cotton gauze) was soaked in 8 mL of ultrapure water, 0.5 mL of the Folin and Ciocalteu reagent (2 M with respect to acid) and 1.5 mL of Na_2CO_3 (20% w/v) for 2 h at room temperature. The absorbance of the solution at 760 nm was quantified by a UV-Vis spectrophotometer and the total polyphenol concentration was estimated in Gallic Acid Equivalents (GAE) with a calibration curve obtained with gallic acid. The same test was performed on release solutions, considering 6 mL of water, 2 mL of the test solution, 0.5 mL of the Folin&Ciocalteu reagent and 1.5 mL of Na_2CO_3 as samples to be analyzed.

3.3.4. Condensed tannin content (CTC) assay

Sections of 1 cm^2 total surface area of the functionalized NF (ker, ker_GPE_ac and ker_GPE_neu) were dipped in a solution consisting of 1 mL of 1% vanillin in methanol and 1 mL of 9 M HCl (2.3 mg of fiber/mL assay solution). The mixture was incubated at 30 °C for 24 h. Finally, the absorbance at 505 nm was measured. Results were expressed as catechin equivalents [33].

3.3.5. 2,2-Diphenyl−1-picrylhydrazyl (DPPH) assay

The assay was performed as previously described with slight modifications [34]. ker_PE_ac, ker_PE_neu, ker_GPE_ac and ker_GPE_neu samples (sections of 1 cm^2 total surface area of the functionalized NF, one sample for each type of surfaces) were immersed in a solution of 50 μM DPPH in ethanol (23 mg of fiber/mL) and the antioxidant power was evaluated by UV–vis spectroscopy measuring the absorbance of the solution at 515 nm over time up to 24 h. In the control experiment, the DPPH assay was run on a pristine keratin NFs (ker). Values are expressed as a percentage of DPPH consumption over time.

3.3.6. Ferric reducing/antioxidant power (FRAP) assay

The assay was performed as previously described with slight modifications [35]. Briefly, ker_PE_ac, ker_PE_neu, ker_GPE_ac and ker_GPE_neu samples (sections of 1 cm^2 total surface area of the functionalized NF, one sample for each type of surfaces) were immersed into a solution of the FRAP reagent (2.3 mg of fiber/mL), containing 0.3 M acetate buffer (pH = 3.6), 10 mM TPTZ and 20 mM ferric chloride (10:1:1 v/v/v ratio). The absorbance of the solution at 593 nm was measured over time up to 3 h. Values are expressed as absorbance of the Fe^{2+}-TPTZ complex over time. In control experiments, the FRAP assay was run on pristine ker.

3.3.7. Cupric reducing antioxidant capacity (CUPRAC) assay

ker_PE_ac, ker_PE_neu, ker_GPE_ac and ker_GPE_neu samples (sections of 1 cm^2 total surface area of the functionalized NF, one sample for each type of surfaces) were immersed into a solution containing $CuCl_2$ (10 mM), neocuproine (7.5 mM), acetate ammonium buffer (1 M at pH 7), and water (1:1:1:0.9 v/v ratio) (2.3 mg of NFs/mL) [36]. The absorbance of each solution at 450 nm was periodically analyzed up to 24 h. In the control experiments, the CUPRAC assay was run on pristine ker.

3.4. Cytocompatibility evaluation

3.4.1. Cell growth conditions

Human gingival fibroblast (HGF) cells (PCS−201–018) were obtained from Promo Cell and cultured in Minimal Essential Medium Eagle-alpha modification (α-MEM; Sigma-Aldrich, Milan, Italy) supplemented with 10% Fetal Bovine Serum (FBS; Sigma-Aldrich, Milan, Italy) and 1% antibiotics. Cells were maintained at 37 °C in a humidified atmosphere containing 5% CO_2 until they reached 80–90% confluence. They were then detached using a 0.25% trypsin-EDTA solution in Phosphate-Buffered Solution (PBS), collected, and used for subsequent experiments. HGF were here applied for wound healing studied due to their origin from highly regenerative connective tissue and their recognized sensitivity to redox-dependent signaling [37,38], making them suitable candidates for healing and antioxidant studies.

3.4.2. Direct cytocompatibility assay

The direct cytocompatibility of ker_PE_ac, ker_PE_neu, ker_GPE_ac and ker_GPE_neu samples was evaluated using HGF; although in the real application scenario it is not expected that the cells will colonize the bandage, the test was done to exclude toxic effects due to direct contact of the bandages on the tissue. Briefly, 50 μL of α-MEM including 15000 cells was seeded onto each sample and incubated at 37 °C for 4 h to allow cell attachment. Subsequently, 500 μL of fresh culture medium was added, and the samples were incubated at 37 °C for 24 h. After incubation, cell metabolic activity and morphology were assessed using an AlmarBlue™ assay (ready-to-use solution, Life Technologies, Milan, Italy) and a scanning electron microscope (SEM; JSM-IT500, JEOL; Tokyo, Japan), respectively. For metabolic activity, the culture medium was replaced with 500 μL of the AlamarBlue™ reagent (0.015% in PBS) and incubated in the dark for 4 h. During this time, metabolically active HGFs reduced resazurin to resorufin, generating a fluorescent signal. Fluorescence was measured with a spectrophotometer (Spark, Tecan, Switzerland) at 530 nm excitation and 590 nm emission, and results were expressed as relative fluorescence units (RFU). For SEM analysis, the samples were fixed with 2.5% glutaraldehyde, dehydrated in graded ethanol solutions (70% and 90%, 1 h for each and 100% for 2 h), mounted on stubs, and sputter-coated with gold for 2 min (Smart Coater, JEOL; Tokyo, Japan) before imaging [39]. Post-analyses of the SEM images, such as the measurement of the cells' dimensions and the percentage of surface area occupied by cells were performed using ImageJ software (v.1.53t).

3.4.3. Indirect cytocompatibility assay

The potential cytotoxic effects of grape and pomegranate agri-food extracts released from ker_PE_ac, ker_PE_neu, ker_GPE_ac and ker_GPE_neu samples on HGF cells were assessed through an indirect cytocompatibility assay, following the International Organization for Standardization (ISO 10993–5 and ISO 10993–12). This test was done to simulate the biological effects of the active ingredients that in the real scenario are released from the bandage onto the healing wound. The samples were immersed in 1 mL of serum-free α-MEM and incubated at 37 °C under agitation (200 rpm) for 7 days. The resulting supernatants were collected and used as conditioned medium for HGF culture. After 24 h of incubation, the cell metabolic activity was determined using the AlamarBlue™ assay, as described previously.

To further evaluate cytotoxicity, activity of the cytosolic enzyme lactate dehydrogenase (LDH) release was measured using the CyQUANT™ LDH cytotoxicity Assay Kit (C20303; Invitrogen; Milan, Italy). The percentage of cytotoxicity was calculated according to the manufacturer's instructions using the following formula [39]:

$$Cytotoxicity\ (\%) = \left[\frac{compound\ treated\ LDH - Spontaneaus\ LDH}{Maximum\ LDH - Spontaneaus\ LDH}\right] \times 100$$

$$Viability\ (\%) = 100 - cytotoxicity$$

.

Cell viability and morphology were additionally examined using dual-fluorescent staining with Live/Dead reagent (Live/Dead(R) Viability/Cytotoxicity Kit for mammalian cells, L3234; Invitrogen; Milan, Italy) combined with NucBlue™ Live Cell Stain ReadyProbes™ reagent (R37605; Invitrogen; Milan, Italy). Viable cells were visualized by green fluorescence (calcein-AM), dead cells by red fluorescence (ethidium homodimer−1), and cell nuclei by blue fluorescence from NucBlue™. The number and distribution of HGFs in the fluorescent Live/Dead images were analyzed using ImageJ software (v.1.53t) after

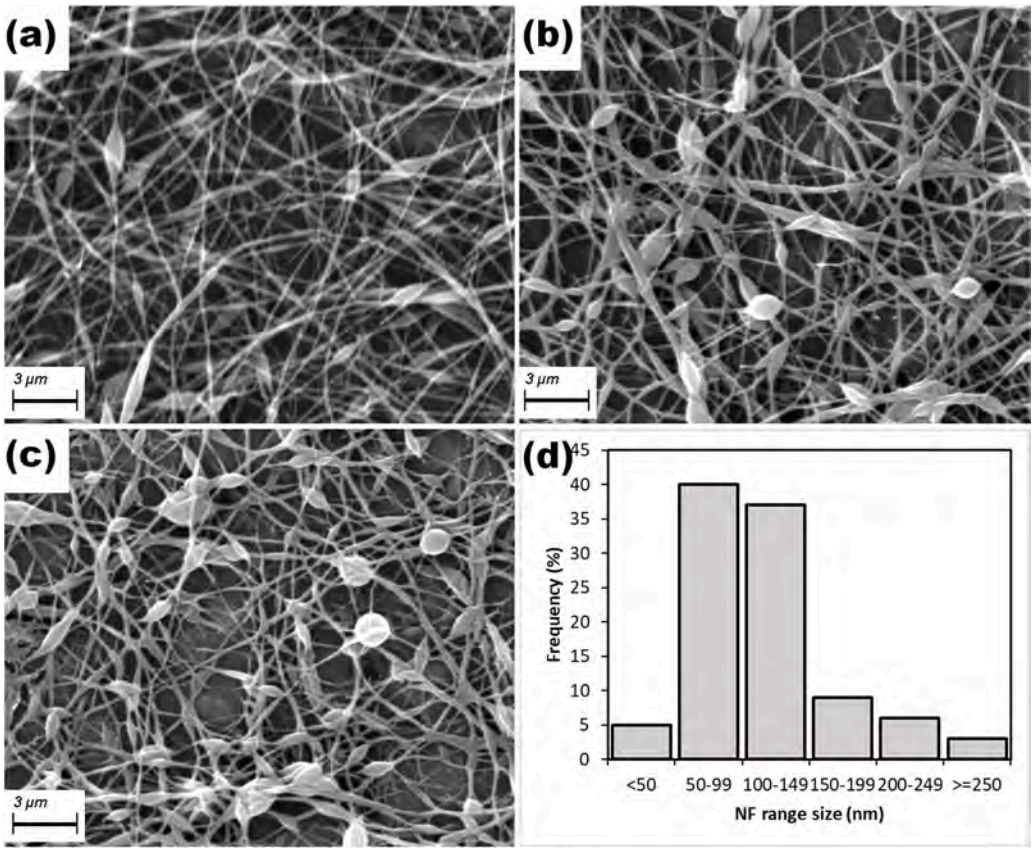


Fig. 1. SEM images of (a) as-spun keratin/PEO NF, (b) keratin/PEO NF after 2 h heating, (c) keratin/PEO NF after 24 h soaking in water, (d) NFs' size distribution. Images magnification= 3000x, bar scale= 3 µm.

background noise reduction and manual threshold adjustment to select cells.

3.5. Antioxidant assessment

The antioxidant potential of the ker_PE_ac, ker_PE_neu, ker_GPE_ac and ker_GPE_neu samples was evaluated by assessing their ability to protect HGFs from intracellular accumulation of toxic reactive oxygen species (ROS) under a chemically induced pro-inflammatory condition. The samples were placed in trans-wells within a 24-well plate, which were in contact with 1 mL of free-serum α-MEM for 3 days at 37 °C to release the polyphenols. The resulting supernatants were then supplemented with 10% FBS and used as culture media for HGFs (15000 cells/well), followed by 24 h of incubation. The day after, oxidative stress was induced by adding 600 µM hydrogen peroxide (H_2O_2) to the culture medium to stimulate intracellular ROS generation as previously demonstrated by the authors [40]. The cells were incubated at 37 °C, and morphology changes were monitored hourly to confirm ROS internalization. ROS production was visualized using CellROX ™ Deep Red Reagent (Thermo Fisher Scientific; Milan, Italy), and fluorescent images were acquired with a Leica TCS SP8 LIGHTNING confocal laser scanning microscope.

3.6. Antibacterial activity evaluation

3.6.1. Bacterial growth conditions

To evaluate the antibacterial activity of ker_PE_ac, ker_PE_neu, ker_GPE_ac and ker_GPE_neu samples, *Staphylococcus epidermidis* was selected, as it is the main concern for wound pathogens. It is a Gram-positive bacterial strain that was purchased from the American Type Culture Collection (ATCC, ATCC 51625, Manassas, Virginia, USA). Bacteria were cultivated on Luria Bertani agar (LB, Invitrogen, Milan, Italy) and incubated at 37 °C until single colonies appeared. Colonies were suspended in 20 mL of LB broth (Invitrogen, Milan, Italy) and incubated overnight at 37 °C under agitation (200 rpm). Prior to the experiment, a fresh subculture was prepared to achieve bacteria in the exponential growth phase. The bacterial suspension was diluted into fresh LB broth to a final concentration of 1×10^3 colony-forming unit (CFU)/mL, corresponding to the optical density (OD) of 0.00001 at 600 nm determined by a spectrophotometer (Spark, Tecan, Switzerland). Fresh LB medium was used as a blank to normalize the OD values.

3.6.2. Antibacterial activity

The antibacterial activity of the ker_PE_ac, ker_PE_neu, ker_GPE_ac and ker_GPE_neu samples against bacterial strains was evaluated by immersing them in 500 µL of bacterial suspension containing 1×10^3 CFU/mL and incubating at 37 °C for 24 h. After incubation, both the activity and the number of bacteria adhered to the dressing surfaces and those remaining planktonic in the culture medium were analyzed, revealing direct effects of polyphenols on surface-attached bacteria and indirect effects of polyphenols released from the dressings on planktonic cells.

To evaluate the surface-adhered bacteria, their metabolic activity and the morphology of bacterial aggregates and cells were examined using the colorimetric AlmarBlue™ assay (0.0015% in PBS) and SEM imaging, as described in Section 2.6.2. Bacterial colorization for SEM observation was performed using SMILE VIEW™ Map 8.2.9621 software.

To assess the viability and enumeration of bacterial colonies in planktonic form, the fluorescent Live/Dead assay (BacLight™, Bacterial Viability Kit for microscopy, Invitrogen, Milan, Italy) and CFU counting

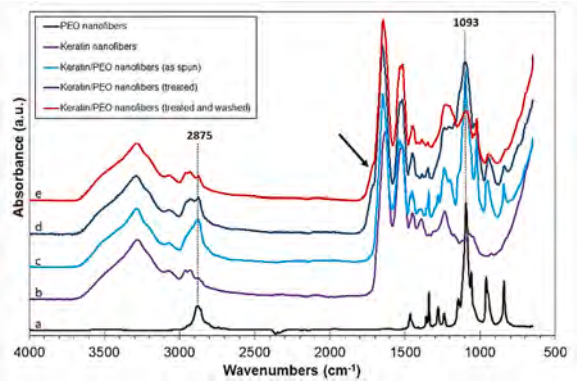


Fig. 2. FT-IR spectra refer to (a) pure electrospun PEO NF, (b) pure electrospun keratin NF, (c) as-spun keratin/PEO NF, (d) keratin/PEO NF after 2 h heating, (e) and keratin/PEO NF after 2 h heating and after 24 h soaking in water. The arrow indicates the shoulder generated after thermal treatment, which is stable after washing, too.

were performed, respectively. In the Live/Dead assay, viable bacterial cells were stained green, and fluorescence images were acquired with an Evois Floid microscope. Post-analysis, including bacterial cell counting, was conducted using ImageJ software (v.1.53t) after background noise reduction and manual threshold adjustment to select the bacterial cells. For CFU determination, bacteria were detached from the dressing surfaces through sonication (5 min, repeated three times) and vortexing (20 s, repeated three times). Aliquots of 200 μL from the detached bacterial suspensions were transferred into a sterile 96-well plate, followed by six consecutive tenfold serial dilutions (20 μL bacterial suspension + 180 μL PBS). Then, 20 μL of each dilution was spotted onto LB agar plates and incubated at 37 °C for 24 h until the bacterial colonies appeared. The number of CFU was calculated using the following formula [39]:

$$CFU = (number\ of\ bacterial\ colonies \times dilution\ factor)\hat{}serial\ dilution$$

.

3.7. Statistical data analysis

Physical-chemical, anti-oxidant and biological characterizations were performed using triplicates. Data are reported as means ± standard deviation (SD). Statistical analysis was performed using SPSS software (v20.0, IBM, Armonk, NY, USA). The Shapiro–Wilk test confirmed the normal distribution of data, and the Levene test verified homogeneity of variance. Subsequently, one-way ANOVA followed by Tukey's post-hoc test was applied to determine differences among groups. Values of $p < 0.05$ were considered statistically significant, unless otherwise specified.

4. Results and discussion

4.1. Keratin NF characterization

Keratin was extracted from Australian Merino wool through a sulfitolysis process, which involved the cleavage of disulfide covalent bonds (RS-SR) into cysteine (R-SH) and cysteine-S-sulfonates (RS-SO_3H). A water-based keratin and PEO solution was prepared to produce keratin NF *via* electrospinning. PEO is a biocompatible water-soluble polymer used to improve the mechanical properties of keratin and enhance electrospinnability. Accordingly, keratin NF was successfully produced from wool-derived keratin using a green approach by a sustainable process. Optimal electrospinning conditions were determined, leading

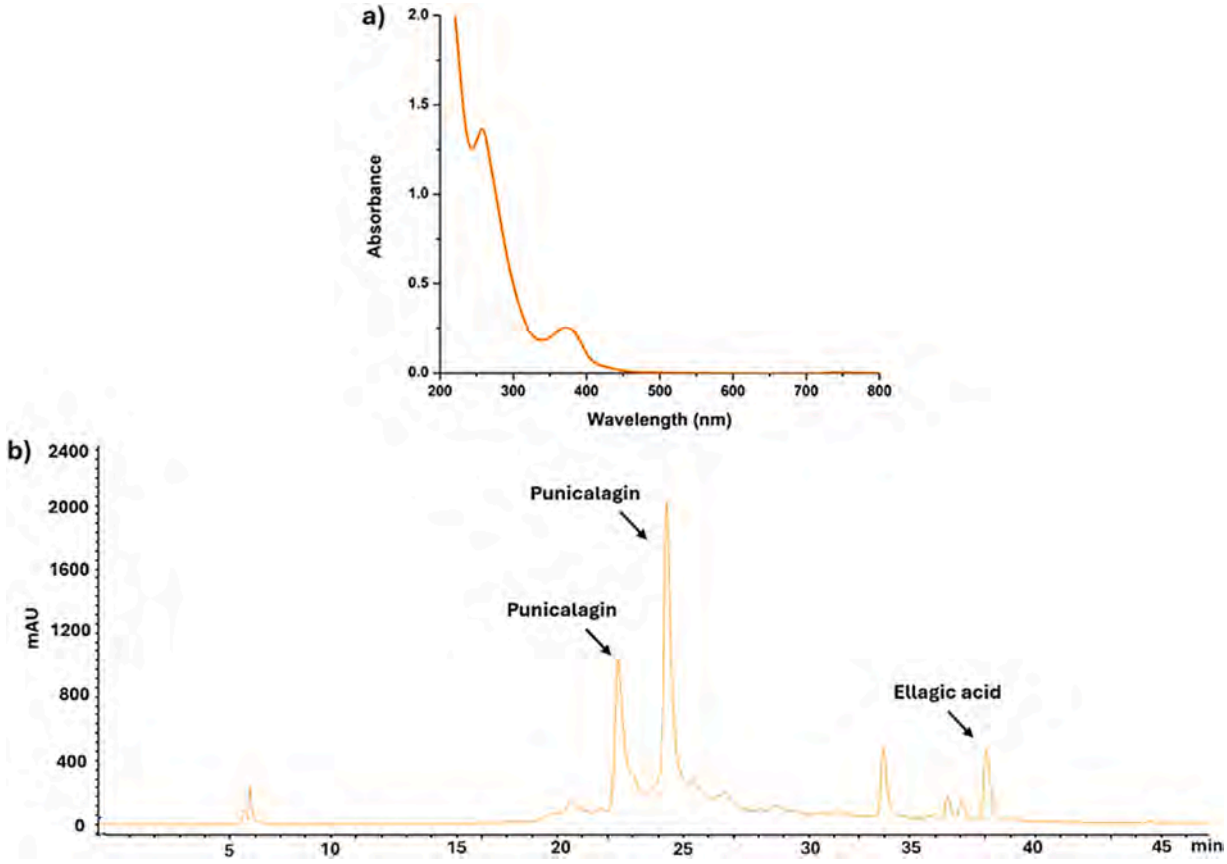


Fig. 3. (a) UV–Vis spectrum of PE (0.5 mg/mL in water); (b) elutographic profile of PE (5 mg/mL).

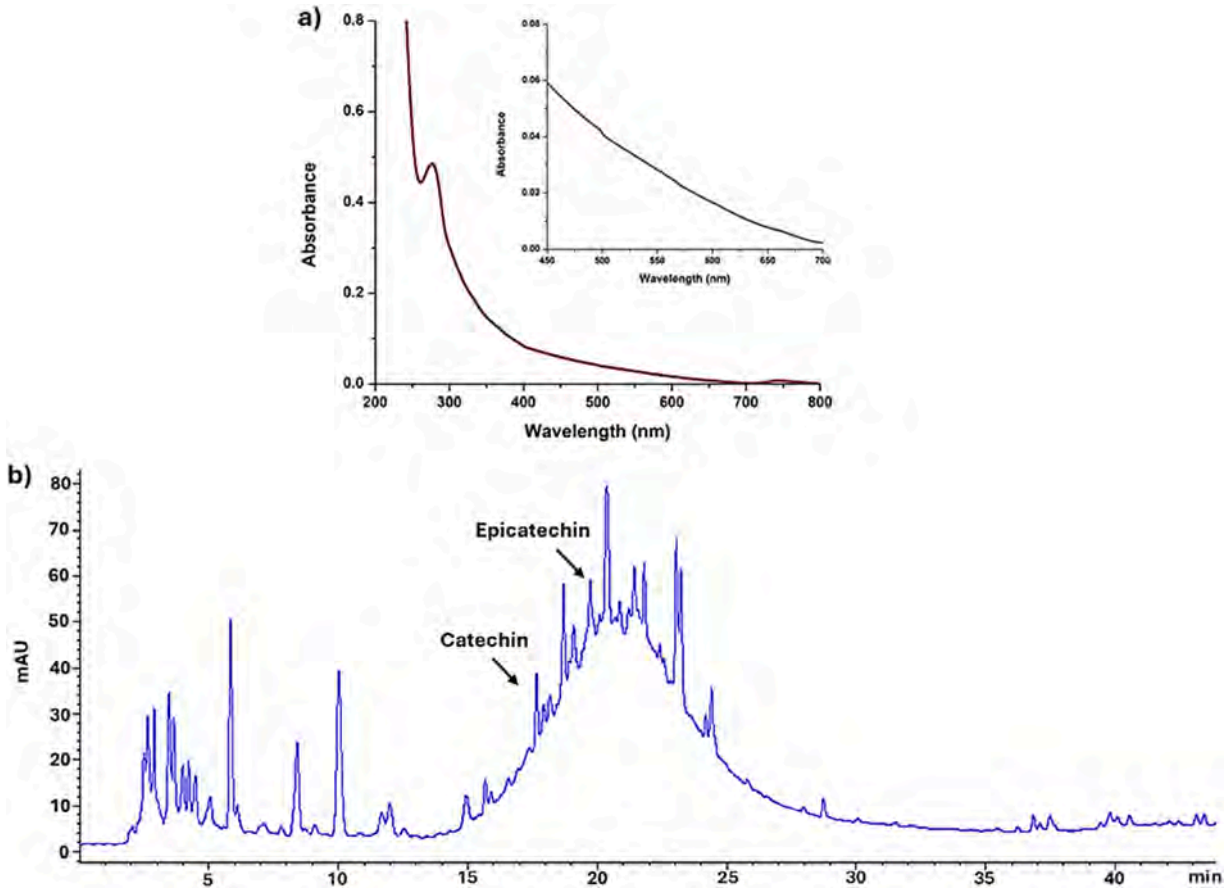


Fig. 4. (a) UV–Vis spectrum of GPE (1.5 mg/mL in water); (b) elutographic profile of GPE (16 mg/mL).

to the successful production of the desired keratin NF. Electrospinning was successfully performed on substrates, including untreated gauze, glass slides and even plasma-treated gauze and glass. Plasma treatment could, in fact, enhance the adhesion between keratin and the substrates [28].

Keratin NF membranes were then further characterized by FT-IR and SEM. SEM analysis was carried out to estimate the diameter of the NF membranes and verify the quality of the NFs. As shown in Fig. 1**a-c**, the NFs displayed a nanoscale diameter as well as they are uniform, despite the presence of some random beads. Similar results were obtained by the Authors in previous works, showing that the selected keratin/PEO ratio of 70:30 is the best compromise between high keratin content and number of beads, as well as proper mechanical properties were achieved although the presence of such random beads [6,27]. The mean diameter of NF after stabilization and soaking was 114.6 ± 50.9 nm (results of 100 measurements from SEM images, Fig. 1**d**). The morphology did not change after heating and soaking in water.

Regarding the FT-IR analysis (Fig. 2), the main absorption bands characteristic of keratin NF (purple line = b) were consistently observed in all keratin/PEO NF samples (light blue line = c; blue line = d; red line = e). In particular, keratin-based NF have absorption bands related to peptide bonds [5]. The amide A band in the range 3100–3700 cm^{-1} is assigned to the stretching vibrations of N = H bonds, the amide I sharp band at 1610 cm^{-1} is assigned to the stretching vibrations of C═O bonds, the amide II at 1520 cm^{-1} is assigned to the bending modes of N—H bonds with contributions of stretching vibrations of C═N groups, and the amide III at 1226 cm^{-1} is the results of N—H bending, C═N stretching vibrations, C—C stretching, and C═O bending vibrations with contributions of hydrogen bonding [41]. The band at 1038 cm^{-1} is attributed to the vibrations of the Bunte's salt residues (C–S–SO_3^-) and cysteic acid [42,43]. Notably, the prominent absorption bands of PEO (black line = a) at 2875 cm^{-1} (C–H stretching vibrations) and 1093 cm^{-1} (C–O–C stretching vibrations) were significantly reduced following heat treatment and subsequent water washing (red line, e), indicating effective removal of PEO [5]. Additionally, a shoulder at 1747 cm^{-1} appeared after the heat treatment (blue line = d), which can be attributed to keratin crosslinking [44]. This feature persisted even after the washing step (red line, e), as observed in Fig. 2, indicated by the arrow, suggesting the structural integrity of the crosslinked keratin network.

4.2. Preparation and characterization of PE and GPE

PE and GPE solutions were prepared by extracting pomegranate waste or grape pomace with water that was selected as the extraction solvent considering the intended use of PE and GPE in the preparation of bioactive gauze for wound care, thus requiring biocompatibility. The extraction yields for each by-product were evaluated based on the quantitation of the solid residues after lyophilization as the presence of sugar components hindered the complete drying of the extracts. The composition of PE and GPE was then investigated by UV-Vis spectroscopy and LC-MS analysis. In the case of PE, the UV-Vis spectrum featured two absorption maxima at 260 and 375 nm (Fig. 3**a**), consistent with the presence of ellagic acid and/or ellagitannins (*e.g.*, punicalagin and punicalin), which are known to be abundant constituent of pomegranate by-products [45]. LC-UV-MS analysis (Fig. 3**b**) showed the presence of three main peaks eluted at *ca.* 22.8, 25.0, and 38.2 min. The peak at 38.2 min was assigned to ellagic acid by comparison with an authentic standard. Quantitative LC-UV-MS analysis indicated an ellagic acid content of *ca.* 5% w/w in the extract. The peaks eluted at 22.8 and 25.0 min were tentatively assigned to punicalagin isomers based on their UV and MS profiles and on comparison with literature data

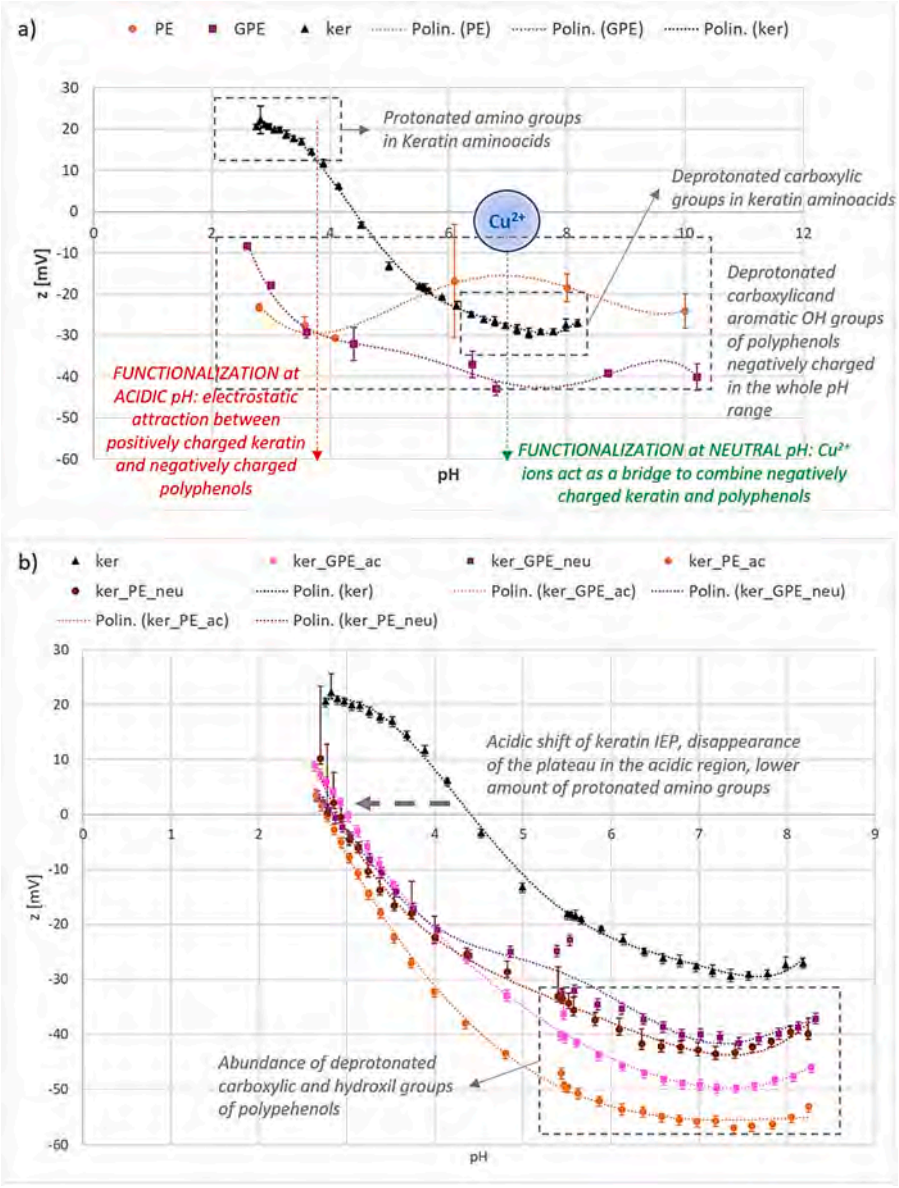


Fig. 5. Zeta potential titration curves of (a) polyphenolic extracts and keratin NF (ker, onto glass substrate), (b) keratin NF (onto glass substrates) before and after functionalization. Points represent experimental data, while lines are polynomial fitting of the data trend.

reported for pomegranate peel extracts [45,46].

As to GPE, condensed tannins (proanthocyanidins) represent the main class of polyphenols present in grape pomace, together with phenolic acids and flavonoids (mainly catechin and epicatechin) as well as anthocyanins [47]. Accordingly, the UV-Vis spectrum of GPE featured an absorption maximum at 280 nm (Fig. 4**a**), indicative of the presence of phenolic compounds, whereas the absorption maximum in the range 450–700 nm could be most reasonably due to anthocyanins. HPLC analysis (Fig. 4**b**) revealed the presence of two main compounds, eluted at *ca.* 19 and 23 min, identified as catechin and epicatechin, respectively, by comparison to authentic standards. Both compounds were present at ~2% w/w, as determined by quantitative HPLC analysis. The broad peak eluted between 15 and 28 min suggested instead the presence of non-chromatographable polymeric compounds, most likely condensed tannins, in agreement with previous data reported in literature [46,48].

The obtained extracts were used to functionalize the keratin NF in order to confer bioactivity, intended as antibacterial and antioxidant properties. Accordingly, Fig. 5 shows zeta potential titration curves of polyphenolic solutions and keratin NF (ker) before and after their functionalization.

The isoelectric point of keratin NF deposited on glass was 4.5 (Fig. 5**a**), as reported in literature for keratin [5], and slightly higher than the one previously measured by the authors on keratin coatings on titanium substrates [49]. The zeta potential titration curve of keratin NF on glass showed a small plateau in the acidic region and another one in the basic region, attributable to basic amino groups and acidic carboxylic groups of keratin amino acids, respectively.

The zeta potential titration curves of polyphenolic extracts (PE and GPE) were well defined, confirming the formation of a colloidal suspension of polyphenolic molecules, and were negative for the whole pH range, showing an acidic behaviour of the functional groups of compounds in the extracts, in accordance with the abundance of carboxylic and aromatic OH groups in polyphenolic molecules (Fig. 5**a**).

The pH of extracts (both PE and GPE) dissolved in water was around 3.7. At this pH, keratin had a moderate positive charge, due to protonated amino groups of some amino acids, while polyphenols were negatively charged, suggesting a potential electrostatic attraction when

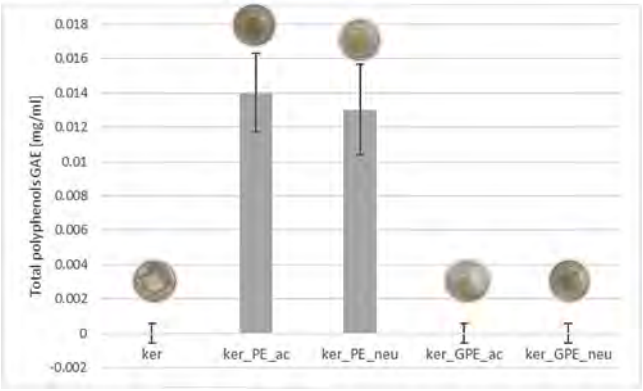


Fig. 6. Folin&Ciocalteu test on solid samples (TCP) before and after functionalization in a neutral (neu) or acidic (ac) environment and visual appearance of the samples. Bars represent means ± SD of n = 3 replicates.

Table 2
Condensed tannin content of GPE. Values are means ± SD (n = 2).

	CTC assay (μg CA/mg NF)
Ker	-
ker_GPE_ac	1.3 ± 0.1
Ker_GPE_neu	10.6 ± 0.1

functionalization is performed in water as a solvent. On the other hand, in neutral conditions (pH close to 7), both polyphenols and keratin were negatively charged (due to deprotonated carboxylic and hydroxyl groups), suggesting that electrostatic attraction cannot be applied for functionalization in this condition. In order to explore dressing processing also at neutral pH, TRIS/HCl buffer (pH 7.4) was used as the medium for polyphenol dilution and Cu^{2+} ions were added to the buffered solution in order to act as a bridge between polyphenols and keratin. In fact, keratin has a high affinity for copper ions and polyphenols have a strong ability to chelate metal ions [5]. In this way, it can be supposed that negatively charged keratin can bind Cu^{2+} ions and attract polyphenol molecules from the solution, at neutral pH. The possibility of applying bivalent metal ions as bridges for polyphenols grafting to negatively charged surfaces was previously explored by the authors using Ca^{2+} ions for polyphenols' grafting on titanium surfaces [30]. The efficacy of the functionalization process was confirmed by zeta potential measurements. As shown in Fig. 5**b**, the isoelectric point of the functionalized keratin was shifted towards more acidic values (2.77 for keratin functionalized with PE in acidic conditions – ker_PE_ac, 2.9 for keratin functionalized with PE in neutral conditions – ker_GPE_neu, 3.00 for keratin functionalized with GPE in acidic conditions – ker_GPE_ac and 2.84 for keratin functionalized with grape in neutral conditions – ker_PE_neu). The plateau in the acidic region (attributable to basic NH_2 groups in keratin) disappeared and the one in the basic region (attributable to acidic functionalities) became more evident, suggesting the presence of abundant acidic OH groups from grafted polyphenols.

The quantification of total polyphenols on keratin NF by means of the Folin&Ciocalteu tests (TPC) is shown in Fig. 6 together with the visual appearance of the samples. Bare keratin did not exhibit any redox response in the test, indicating the absence of interference with the assay. Conversely, a significant polyphenol content was detected on

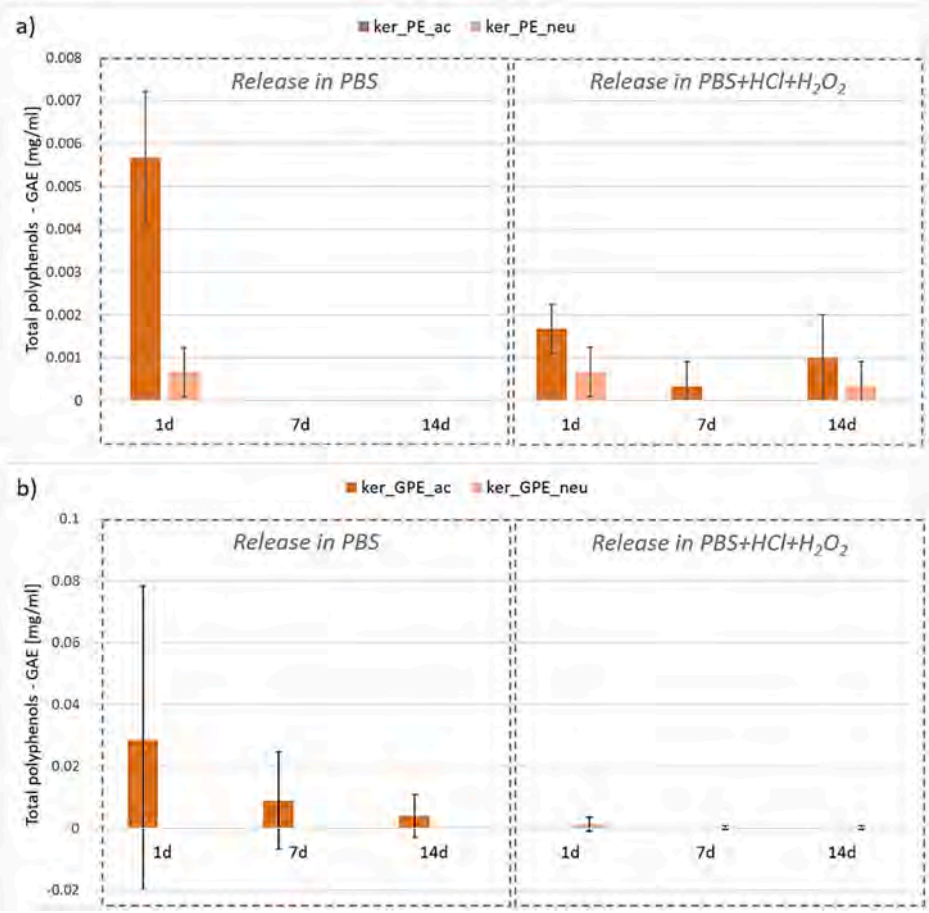


Fig. 7. Total polyphenol quantification by means of the Folin&Ciocalteu test on release solutions of keratin functionalized with (a) PE and (b) GPE. Bars represent means ± SD of n = 3 replicates.

Table 3
Summary of the physico-chemical characterizations. ✓ (presence, qualitative), x (absence), + (moderate presence), ++ (high presence), - (not applicable).

	z-pot	Release (neutral pH)	Release (inflamm. pH)	F&C	CTC	DPPH	FRAP	CUPRAC
Ker_PE_ac	✓	++	+	++	-	++	++	++
Ker_PE_neu	✓	++	+	++	-	++	++	++
Ker_GPE_ac	✓	+	x	x	+	++	++	+
Ker_GPE_neu	✓	+	x	x	++	+	+	+

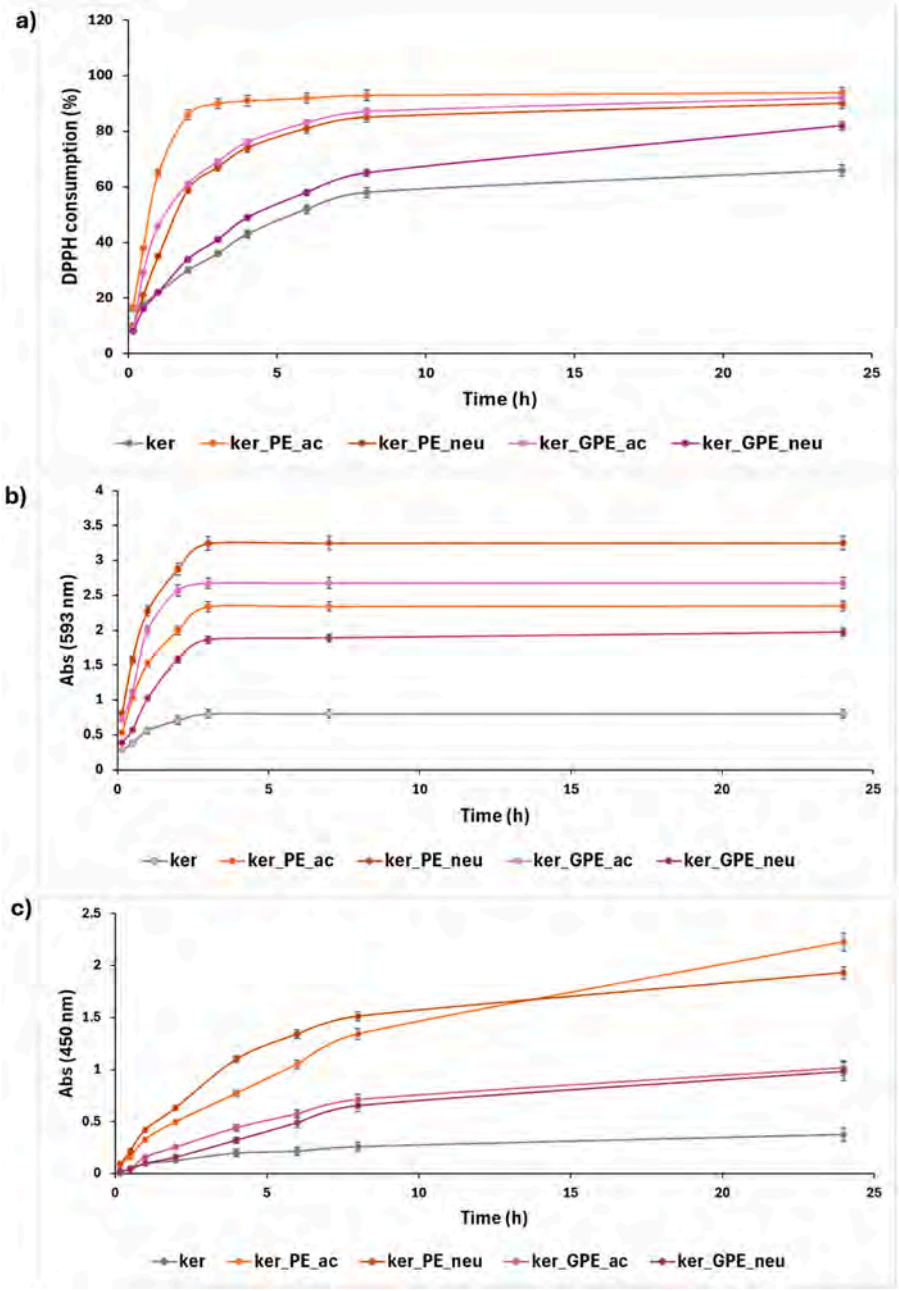


Fig. 8. (a) DPPH reducing activity, (b) Fe^{3+} reducing activity and (c) Cu^{2+} reducing activity of PE and GPE functionalized keratin NF. Bars represent means ± SD of n = 2 replicates.

keratin functionalized with PE, under both acidic and neutral conditions, confirming the effective functionalization. No measurable signal was observed for keratin functionalized with GPE, likely due to the lower reactivity of GPE components toward the FC reagent. Therefore, considering that GPE is generally rich in condensed tannins, GPE-functionalized NFs were further characterized by the condensed tannin content assay.

The visual appearance of the samples reveals fibers' colouring after functionalization. Data reported in Table 2 confirmed the presence of condensed tannins and a larger amount of them on the sample functionalized at neutral pH, confirming that the NFs functionalization was effective even with GPE.

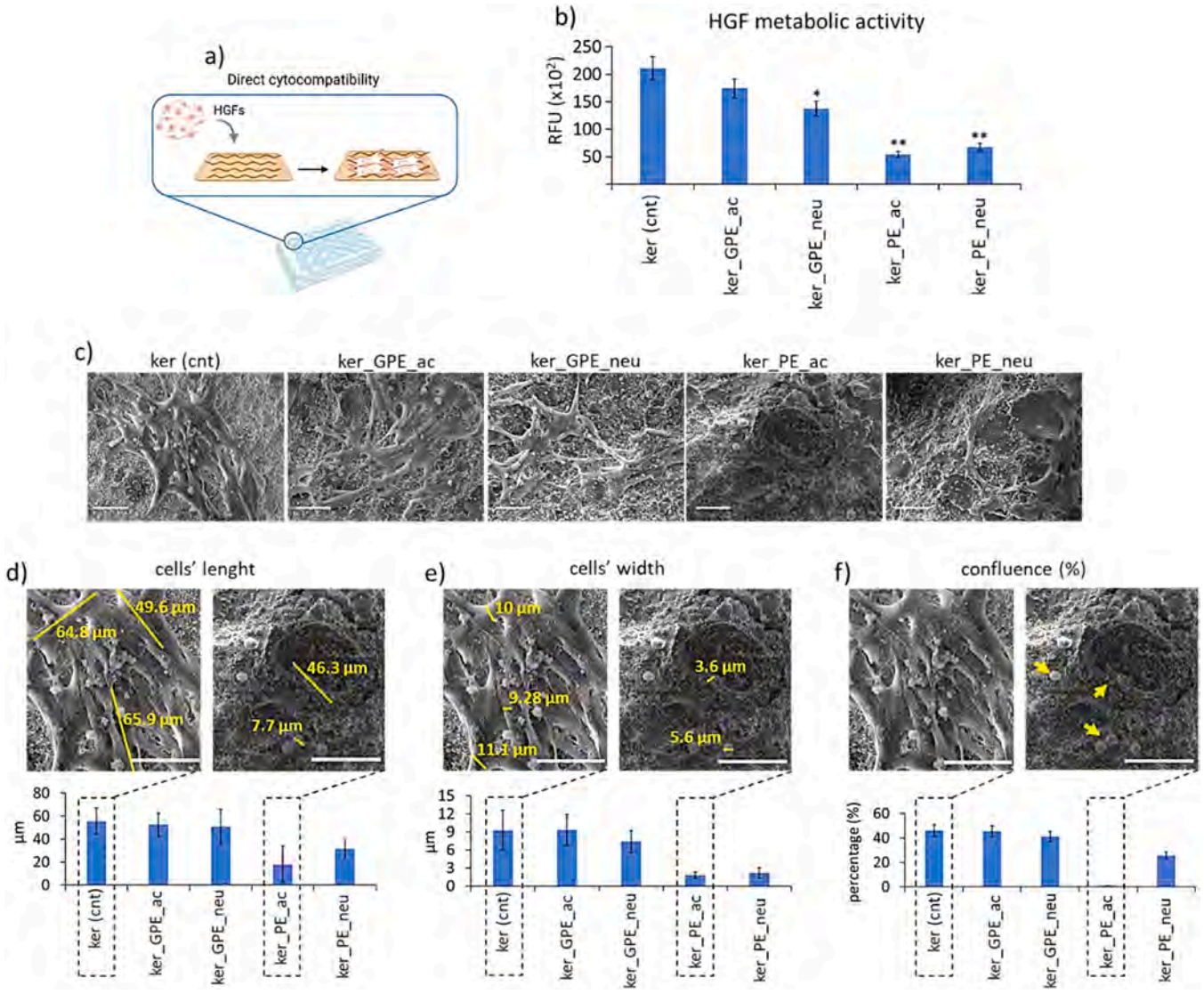


Fig. 9. Direct cytocompatibility evaluation of polyphenol-doped dressings toward HGFs after 24 h of incubation. (a) Schematic representation of the experimental design; (b) Metabolic activity of surface-adhered cells, * and ** indicate $p < 0.05$ and $p < 0.01$, respectively; (c) SEM images of cell morphology; (d-f) Quantitative analysis of cell dimensions using ImageJ software (v. 1.53 t), SEM scale bar= 50 µm. Bars represent means ± SD of n = 3 replicates.

Polyphenol release from functionalized keratin nanofibers was investigated under physiological (Release in PBS) and pro-inflammatory pH (Release in PBS+HCl+H_2O_2) conditions (Fig. 7). Eluates from keratin functionalized with PE (Fig. 7**a**) exhibited a burst release within the first day (for samples functionalized in both pH conditions) when release occurred at physiological pH, whereas a lower and more gradual release profile was observed under inflammatory pH conditions. Eluates from NFs functionalized with GPE (Fig. 7**b**) showed a detectable polyphenol release only when functionalization was performed under acidic conditions, with higher release at physiological pH compared to pro-inflammatory pH. However, the relatively large variability observed in these data is reflected by the high standard deviations. A higher standard deviation of the release data at day 1 can be explained by considering the presence of a fraction of molecules weakly physically absorbed on the porous dressing, which were poorly reproducible and were easily released at the first immersion. However, the variability was limited for PE functionalized samples, while it was extremely high for GPE ones. Different interpretations can be done for this: the low reactivity of GPE compounds for the Folin&Ciocalteu reagent, previously cited and/or a general higher bonding strength between GPE and keratin. In any case, the trend of the release data (Table 3) seems reasonable and in line with the other functionalization results. In addition, no residual polyphenols were detected on the solid samples at the end of the release tests. All the samples tested in physiological conditions (PBS) were completely intact at the end of the test, on the other hand samples tested in pro-inflammatory conditions were partially degraded evidencing a certain dissolution induced by this solution.

4.3. *Evaluation of the antioxidant properties*

DPPH, FRAP and CUPRAC assays (Fig. 8) showed that the functionalization with both PE and GPE imparted an antioxidant functionality to the keratin NF, which was particularly evident for the PE extract. Indeed, an 86% DPPH reduction was observed with ker_PE_ac already after 2 h, whereas the ker_PE_neu and ker_GPE_ac samples were found to be slightly less active leading to 59% and 61% DPPH reduction, respectively (Fig. 8**a**). The ker_GPE_neu sample was found to be significantly less active, leading to only a 34% DPPH reduction after 4 h; however, an 82% reduction was reached after 24 h. Similar results were observed in the FRAP (Fig. 8**b**) and CUPRAC (Fig. 8**c**) assays, with the functionalized NF with PE exhibiting higher absorbance values than that of the pristine keratin NF at 3 or 24 h, although differences between the

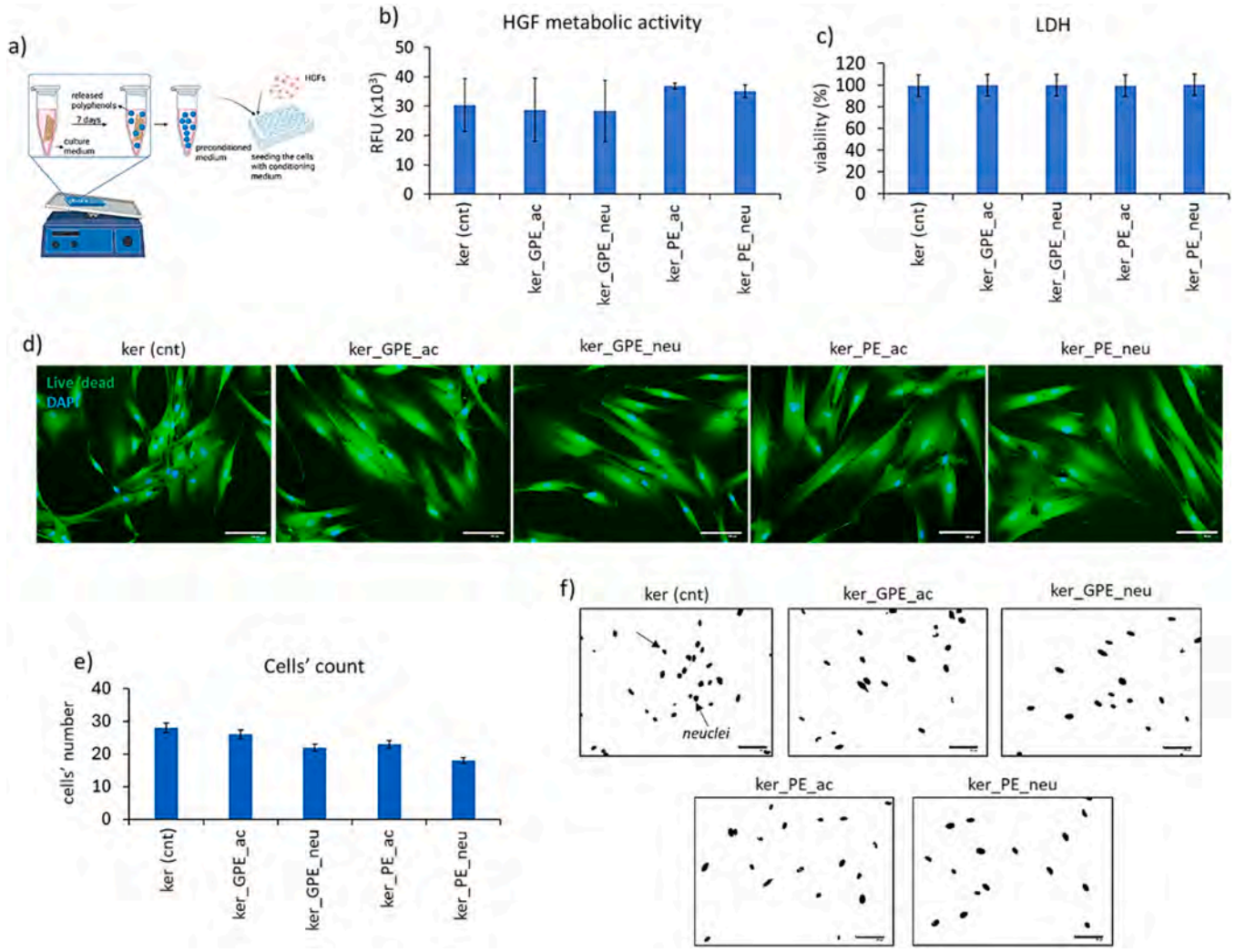


Fig. 10. Indirect cytocompatibility evaluation of polyphenols released from the doped dressings into conditioned media and their effects on HGFs after 24 h of incubation. (a) Schematic representation of the experimental design; (b) Cell metabolic activity; (c) LDH assay results; (d) Dual-fluorescent staining with Live/Dead dye and NucBlue for nuclear visualization; (e-f) Post-analysis of Live/Dead fluorescent images and counting cells' nuclei using ImageJ software. Images bar scale= 100 μm. Bars represent means ± SD of n = 3 replicates.

keratin NF functionalized with the two extracts at different pH were less marked in the FRAP assay. So, it can be speculated that the functionalization was more effective and the release of polyphenols was larger for keratin NF functionalized with PE in acidic conditions, without copper ions as linkers. The functionalization with GPE at neutral pH, with copper ions as linkers, was characterized by the strongest chemical bond of the polyphenols to the keratin NF.

Finally, Table 3 summarizes the evaluation of the presence, activity and release of polyphenols on the various functionalized materials. It is evident that polyphenols (both PE and GPE) have been successfully grafted to keratin fibers both in acidic and neutral conditions, as confirmed by zeta potential titration curves and CTC, DPPH, FRAP and CUPRAC assays. On the contrary, the release of active polyphenols from functionalized samples is significantly different comparing PE and GPE grafted materials and the various grafting conditions, as evidenced by release and Folin&Ciocalteu test. It can be observed that the Folin&Cioocalteu test is particularly sensitive to release polyphenols (comparison between release and total phenol content by Folin&Ciocalteu test) in accordance with a previous investigation by the authors [30].

4.4. Cytocompatibility

Polyphenol-functionalized and control (i.e., polyphenol-free) electrospun dressings were evaluated for their cytocompatibility towards human gingival fibroblasts (HGFs), selected as representative skin-resident cells involved in the early activation of the *in situ* pro-inflammatory cascade. In fact, as previously mentioned in the materials and methods section, HGF provides a well-studied and physiologically relevant model for soft tissue regeneration, originating from highly regenerative connective tissue with active fibroblastic behavior [37,38]. Their primary nature and heightened sensitivity to redox-dependent signaling make them particularly suitable for evaluating the cytotoxic effects of bioactive compounds and cellular redox balance as well.

The direct-contact assay was performed to mimic the interaction between the dressings and soft tissue by seeding HGFs directly onto the dressing surfaces (Fig. 9**a**). The meaning of the direct assay relies on the fact that, although in the real scenario it is not expected that the cells will colonize the bandage, the test was done to exclude toxic effects due to direct contact of the bandages' components with the healing tissue.

The results of the direct-contact assay are presented in Fig. 9**b-f**. The metabolic activity of HGFs cultivated onto the samples' surfaces showed a significant reduction ($p < 0.01$ indicated with **) in contact with

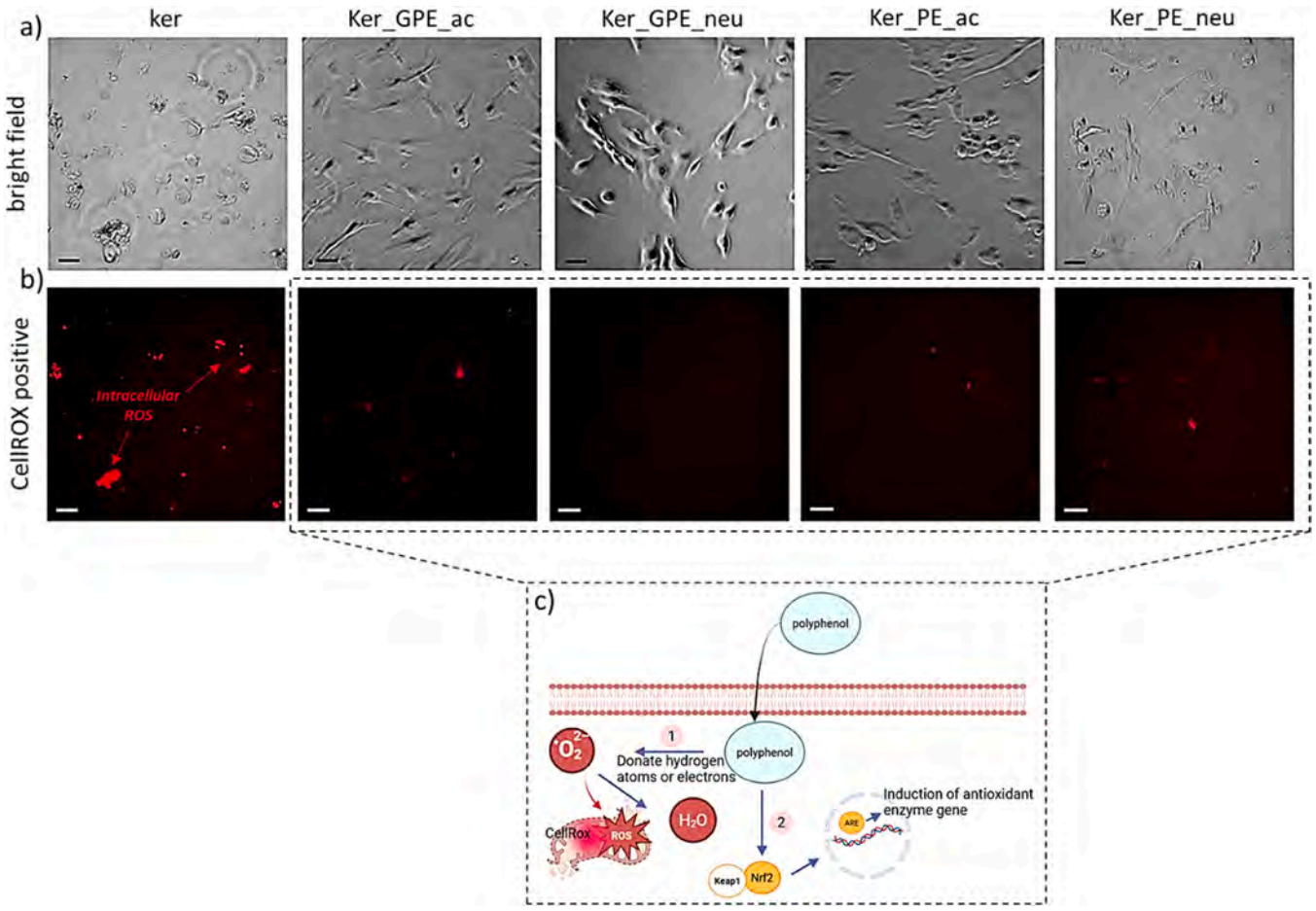


Fig. 11. Evaluation of antioxidant and anti-inflammatory properties of polyphenols released from doped dressings into conditioned media.(a) Cell morphology under oxidative stress induced by H_2O_2; (b) intracellular ROS (red fluorescent) detected using CellRox™ Deep Red reagent; (c) Schematic illustration of the antioxidant mechanisms of polyphenols through two main pathways: 1) donation of hydrogen atoms or electrons to the ROS, converting them into H_2o, and 2) activation of the Nrf2-ARE signalling system, leading to the upregulation of antioxidant enzyme genes. Images bar scale= 20 μm.

ker_PE_ac and ker_PE_neu samples when compared with ker controls. In contrast, the RFU values of cells on ker_GPE_ac and ker_GPE_neu dressings were comparable to those of the control, showing no significant differences (Fig. 9**b**). SEM images (Fig. 9**c**) revealed a physiological fibroblast-like morphology, with well-spread cells on both ker_GPE_ac and ker_GPE_neu dressings. In general, the ability of the electrospun fibers to influence cells' adhesion and spread was previously discussed by the authors [50], suggesting a "contact-guidance" biomechanical instructive process; accordingly, the fibers per se represent the topographic guide for cells that are induced to populate the dressing following the surface's orientation. Here, fewer cells adhered to the ker_PE_neu surface, although those present exhibited normal spread. Conversely, cells on ker_PE_ac surfaces displayed a rounded morphology (indicative of deactivated or apoptotic cells), likely due to the too high amount of grafted/released polyphenols, as evidenced by the physico-chemical characterization. Quantitative SEM analyses performed using ImageJ confirmed a reduction in cell length, width, and the percentage of surface area occupied by cells (calculated as: occupied area × 100/total area), particularly evident for the ker_PE_ac dressing (Fig. 9**d-f**; representative measurements shown). However, following previous work reporting about polyphenol's' influence towards human cells' metabolism [51], we can hypothesize that the observed reduction of metabolic activity is not due to a cytotoxic effect because we are far from the reported toxic concentrations (typically 0.05 – 0.1 mg/mL) [52], but rather to a difficulty in adapting to the amount of molecules grafted onto the surface. In fact, the Folin&Ciocalteu test (Fig. 6) revealed a higher concentration of surface-bonded polyphenols by the PE extract over the GPE one; this represents a key information as previous literature reported about a dose-dependent role of polyphenols in reducing cells' metabolic activity by different pathways such as cyclins expression [53], down-regulation of ERC and SMAD expression [53] and reduced lipid metabolism [54], over a direct toxic effect. Conversely, we do not hypothesize a direct cytotoxic effect of polyphenols since the families of molecules identified are not known to be intrinsically toxic except towards tumor cells [54] or at concentrations much higher than those observed in our functionalization (>100μM) [55].

In addition to evaluating the direct effects of the polyphenol-functionalized dressings on HGF activity and attachment, further experiments were conducted to assess the influence of polyphenols released from the samples on cell behaviour. According to the ISO standards (ISO 10993–5 and ISO 10993–12), conditioned media were prepared by immersing the samples in the culture medium and incubating them under agitation for 7 days. The resulting supernatants (conditioned media) were then used for cell cultivation (Fig. 10**a**). This test was done to simulate the biological effects of the active ingredients that, in the real scenario, are released over days from the bandage into the healing wound, thus representing a simulation of the application.

In general, no significant reduction in the metabolic activity of HGFs cultured with conditioned media from polyphenol-functionalized dressings was observed compared with the ker control samples (Fig. 10**b**). Assessment of lactate dehydrogenase (LDH) release (Fig. 10**c**), a marker of membrane integrity, showed comparable results within all of the tested groups and the control, suggesting no toxic side effects due to the polyphenols release. According to the ISO protocol,

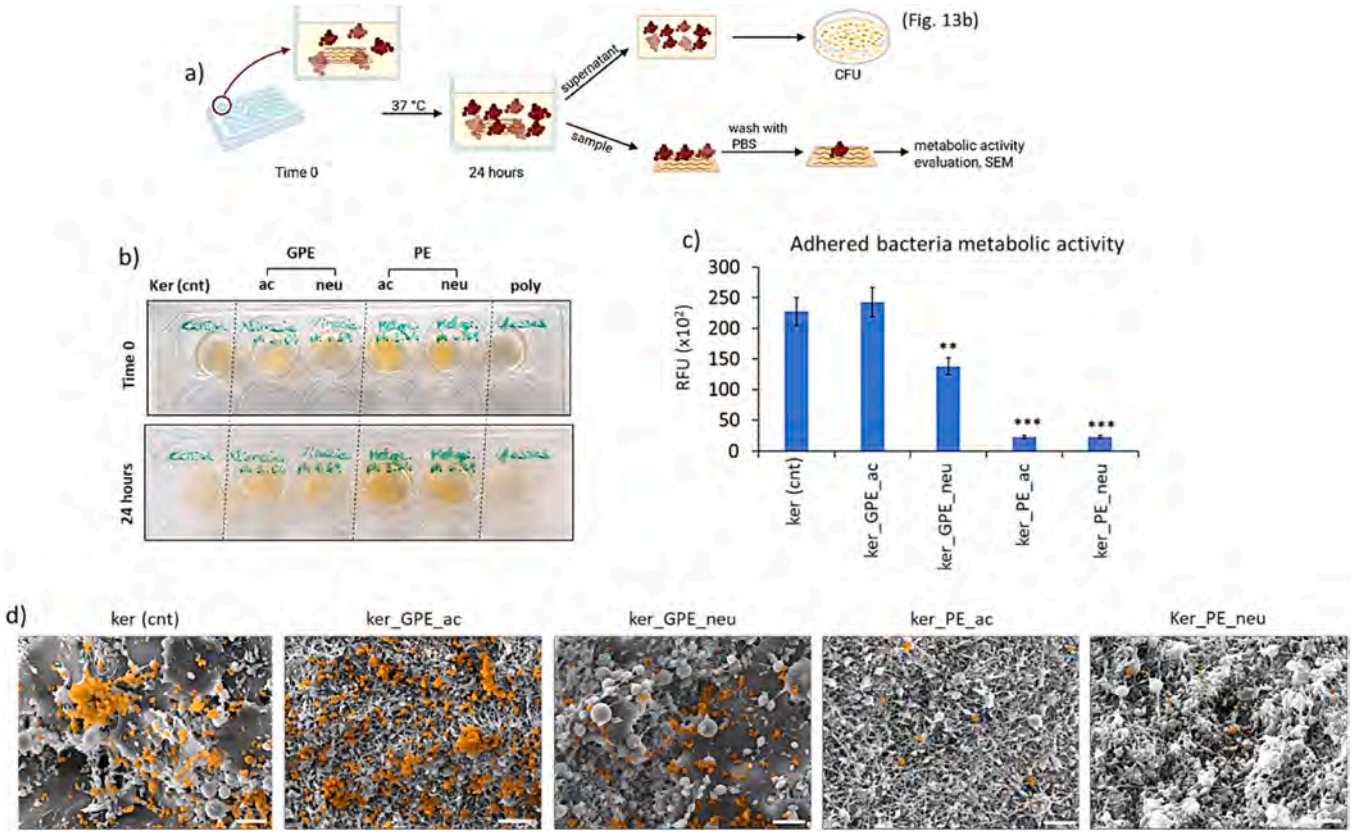


Fig. 12. Evaluation of the antibacterial activity of polyphenol-doped dressings against S. epidermidis. (a) Schematic representation of the experimental design; (b) Turbidity visualization of bacterial growth at time 0 and after 24 h of incubation; (c) Metabolic activity of surface-adhered bacteria, ** and *** indicate $p < 0.01$ and $p < 0.001$, respectively; (d) SEM images of surface-adhered bacteria (bacteria marked by orange color). Images bar scale= 5 μm. Bars represent means ± SD of n = 3 replicates.

cell viability below 70% indicates cytotoxicity. In this study, viability remained around 80% for all of the tested groups, suggesting that even the ker_PE_ac dressings were cytocompatible under indirect conditions. Furthermore, dual-fluorescent staining using the Live/Dead reagent and NucBlue nuclear stain (Fig. 10**d**), combined with ImageJ-based nuclei counting, demonstrated that the majority of cells remained viable and well-spread, with no statistically significant differences in cell numbers (Fig. 10**e-f**).

The complementary use of direct and indirect cytocompatibility assays enables the distinction between surface-driven and release-mediated cellular responses, providing a comprehensive understanding of the biological response to the functionalized dressings. Direct contact effects primarily reflect the influence of mechanical properties, surface chemistry and charge on cell adhesion and spread [56]. Indirect contact well simulates the biological response due to the effect of the released bioactive compounds into the healing site. The results of direct and indirect biological tests suggest that the reduction in cell viability observed for ker_PE_neu and ker_PE_ac can be attributed mainly to a direct contact effect more than to a release-mediated one. Based on these premises, we tend to consider the indirect test more representative for a bioactive bandage, as the tissue should not be expected to grow directly onto the gauze but rather to be influenced by the bioactive factors that are released by the bandage covering the wound. So, following this reasoning, all of the here-developed dressings seem to be appropriate candidates for further investigations.

In general, the observed biocompatibility of dressings functionalized with polyphenols from PE and GPE by-products is consistent with previous findings in the literature. Brezoiu et al., (2019) encapsulated grape pomace polyphenolic extracts within mesoporous silica matrices to improve extract stability and demonstrated high cytocompatibility toward HaCaT human keratinocytes. The results revealed high cytocompatibility of the encapsulated extract into Zn-MCM−41 matrix [57]. Similarly, Motta et al. (2025) reported that dextran-grape conjugates (a grafting reaction between GPE and dextran) exhibited excellent cytocompatibility with both keratinocyte and fibroblast cell lines [58]. Furthermore, Hashemi Poor et al., (2022) investigated the effect of pomegranate peel ethanolic extract (PPE) on human dermal fibroblast, and observed enhanced cell proliferation and migration after 24 h of exposure with 25 μg/mL PPE, as evidenced by MTT and scratch assays [59]. Collectively, these studies support the present results, confirming that polyphenols derived from agri-food by-products maintain favorable biocompatibility and may influence cells' behaviour in the wound-healing processes when incorporated into polymeric dressings or carriers.

4.5. *Antioxidant properties*

Agri-food by-products such as grape pomace and pomegranate peels are rich in diverse polyphenolic compounds, primarily flavonols and catechins in grape and punicalagins (α and β) in pomegranate, as confirmed by UV-Vis and HPLC analyses reported in Figs. 3 and 4, which are recognized for their potent antioxidant and anti-inflammatory properties. Commonly, these effects arise from their ability to scavenge electrons and reduce reactive oxygen species (ROS), as well as to activate the Nrf2-ARE signaling pathway, thereby upregulating antioxidant enzyme genes, as illustrated in Fig. 11**c** [60–62]. To evaluate the antioxidant potential of the polyphenol-functionalized dressings, HGFs were cultured using conditioned media where the oxidative stress was chemically induced with H_2O_2, as detailed in the Section 2.6.4.

The results are presented in Fig. 11**a-b**. The top panel (Fig. 11**a**)

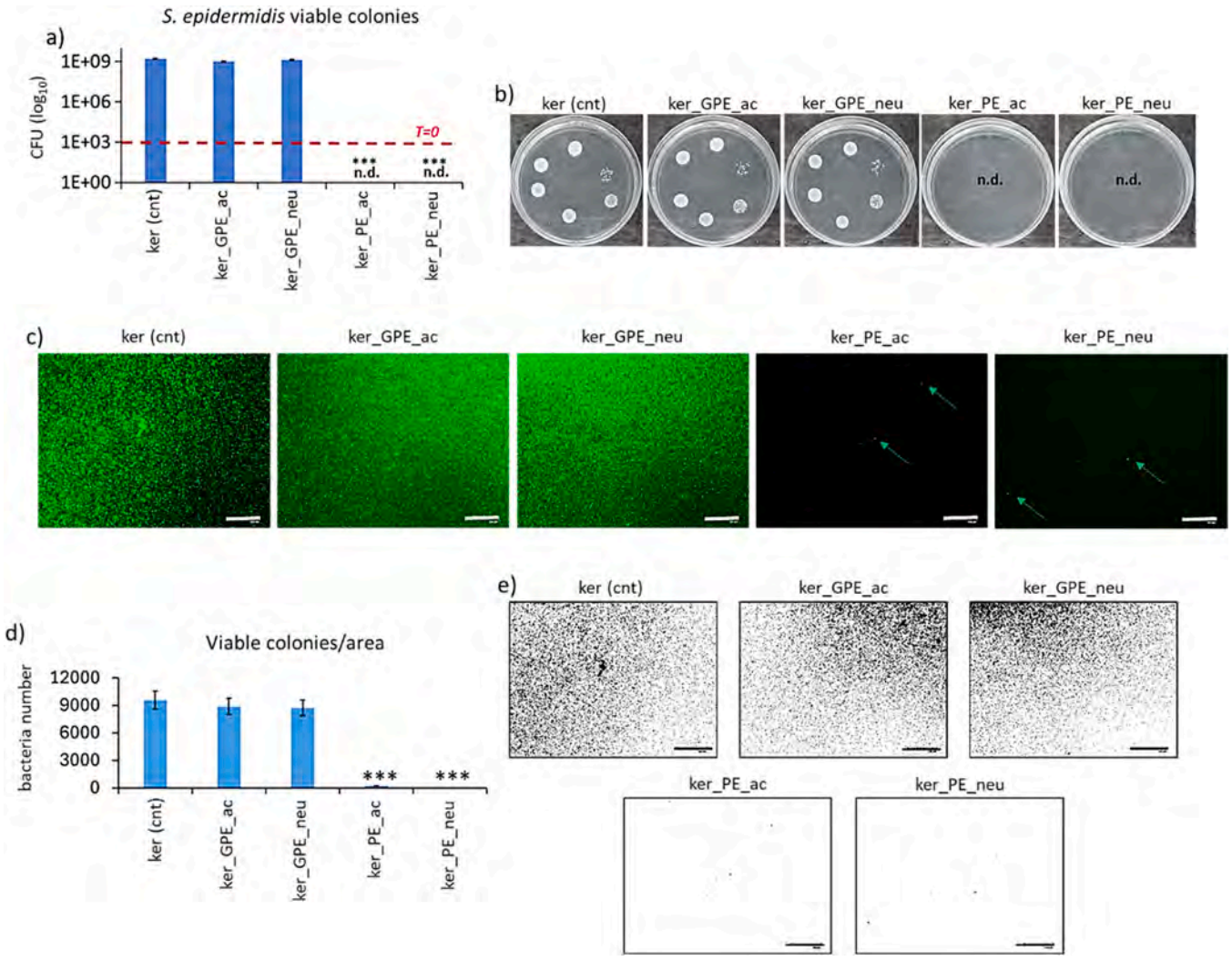


Fig. 13. Evaluation of the antibacterial activity of polyphenol-doped dressings against the planktonic form of S. epidermidis. (a) Enumeration of viable bacterial colonies; (b) Images of CFU plate; (c) Fluorescent Live/Dead staining; (d-e) Post-analysis of Live/Dead fluorescent images by counting bacterial cells using ImageJ software. *** indicates $p < 0.001$, n.d=not detected. Images bar scale= 100 μm. Bars represent means ± SD of n = 3 replicates.

represents cell morphology in brightfield images, while the bottom panel (Fig. 11**b**) shows fluorescent CellROX™ staining, where ROS accumulation is visualized as red fluorescence. Cells cultured with the ker control conditioned medium exhibited morphological signs of oxidative stress, accompanied by strong intracellular red fluorescence, suggesting a strong stress due to the ROS. Conversely, cells maintained a well-spread morphology with markedly reduced ROS fluorescence signals in the presence of polyphenols, demonstrating a significant attenuation of oxidative stress and confirming the antioxidant efficacy of the functionalized dressings. These results suggest that polyphenols released from functionalized dressings are sufficient to exhibit a strong antioxidant activity for all the tested materials, even if the release is not detected by the Folin&Ciocalteu test for some samples.

4.6. Antibacterial properties

After confirming the cytocompatibility and antioxidant properties of the polyphenol-functionalized dressings, further experiments were conducted to assess their antibacterial efficacy against *Staphylococcus epidermidis,* a common Gram-positive pathogen associated with wound infections. Following incubation, bacterial metabolic activity and viability, both for surface-adhered and floating planktonic populations, were quantified using the metabolic AlamarBlue assay and the viable colonies count (CFU) (Fig. 12**a-b**). Additionally, the morphology and distribution of bacterial aggregation were examined by SEM.

After 24 h of incubation, a clear reduction of the turbidity in the bacterial suspension was observed in the presence of ker_PE_ac and ker_PE_neu, suggesting inhibited bacterial growth (Fig. 12**b**). In fact, quantitative analysis revealed a significant decrease in the metabolic activity of the surface-adhered bacteria for both ker_PE_ac and ker_PE_neu ($p < 0.001$ indicated by ***), as well as for ker_GPE_neu ($p < 0.01$ indicated by **), compared with the ker control (Fig. 12**c**). SEM images corroborated these results, showing dense micro-biofilm formation and bacterial clusters on control surfaces, whereas only sparse and isolated colonies were visible on ker_PE_ac and ker_PE_neu samples (Fig. 12**d**). These findings confirm that polyphenols extracted from pomegranate exhibit strong antibacterial activity against *S. epidermidis* in direct contact with the doped dressings, thus ideally protecting the wound site from external infections.

Afterwards, the analysis of the supernatant and the floating planktonic bacteria (Fig. 12**a**) demonstrated an indirect antibacterial effect mediated by polyphenols released from the dressings. CFU plate counts and imaging (Fig. 13**a and b**) revealed the absence of bacterial growth in the supernatant, while Live/Dead fluorescent staining confirmed the presence of only a few viable planktonic cells in the ker_PE_ac and ker_PE_neu samples. Additionally, the counting of bacterial cells on the

Live/Dead fluorescent images demonstrated a significant reduction in the presence of ker_PE_ac and ker_PE_neu dressings. (Fig. 13**d-e**). Such findings seem to be very promising as it can be hypothesized that the release of bioactive compounds from the dressing to the wound site can contribute to the eradication of the infection in the injury site.

The potent antibacterial activity observed for PE-functionalized dressings can be mainly attributed to the high content of hydrolysable ellagitannins and ellagic acid, which are known to exert antibacterial effects through multiple mechanisms including bacterial membranes disrupt, increased membrane permeability, chelation of essential ions, and interference with quorum sensing and biofilm formation [63–66]. The complete absence of viable cells in the supernatant further indicates a bactericidal rather than bacteriostatic effect, consistent with the sustained release of active polyphenols from the dressing matrix. In contrast, GPE-functionalized dressings displayed moderate antibacterial activity, likely due to differences in the composition, concentration, and solubility of proanthocyanidins and flavonols [63–66]. Collectively, these findings support the potential of pomegranate-derived polyphenols as sustainable, multifunctional agents for incorporation into biopolymeric wound dressings, providing effective antibacterial and anti-inflammatory activity while aligning with the principles of green chemistry and antimicrobial stewardship.

5. Conclusions

Increasing global waste generation is one of the world's most critical environmental issues. Therefore, finding solutions and technologies that transform waste into valuable resources is necessary. Here we demonstrated that a combination of keratin NFs from discarded wool functionalized with polyphenol-rich solutions extracted from PE and GPE by-products can represent an example of how to valorise local by-products to obtain green, low-cost and bioactive wound dressings matching the desired clinical needs. The extraction of keratin from discarded wool and its subsequent electrospinning, together with the recovery of polyphenols from agri-food by-products, were optimized under environmentally friendly conditions. Then the coupling of keratin NFs with polyphenols was rationally designed based on their physico-chemical affinities, enabling effective and stable functionalization. Preliminary biological evaluations demonstrate the possibility of obtaining cytocompatible, antioxidant and antibacterial biomaterials suitable for wound dressing applications, while also highlighting significant differences in the biological performance of distinct polyphenolic compounds. Among the investigated systems, pomegranate functionalized keratin nanofibers resulted in the most promising materials for the targeted application. The use of recycled raw materials and green processing routes supports the development of new sustainable and low-cost solutions with promising biological properties. Finally, we also acknowledge the limitations of this study regarding the biological characterization that requires further studies to better clarify the molecular mechanisms driving healing and bacteria repulsion by the use of advanced models such as 3D humanized tissues and appropriate animal models as well.

CRediT authorship contribution statement

Erica Savino: Writing – original draft, Methodology, Investigation, Data curation. **Claudia Vineis:** Supervision, Investigation, Funding acquisition, Conceptualization. **Alfieri Maria:** Investigation, Funding acquisition, Conceptualization. **Silvia Spriano:** Writing – review & editing, Supervision, Data curation. **Alessio Varesano:** Writing – original draft, Investigation, Data curation. **Lia Rimondini:** Writing – review & editing, Supervision. **Ziba Najmi:** Writing – original draft, Methodology, Investigation, Data curation. **Sara Ferraris:** Supervision, Investigation, Funding acquisition, Conceptualization. **Andrea Cochis:** Supervision, Investigation, Funding acquisition, Conceptualization.

Declaration of Competing Interest

The authors declare that they have no known competing financial interests or personal relationships that could have appeared to influence the work reported in this paper.

Acknowledgments

This work was carried out within the PROTECTED project (P2022XT785) financed by the European Union through the Next GenerationEU plan, Mission 4, Component C2, Investment 1.1. as part of the PRIN 2022 PNRR Call (D.D.1409 of 14/09/2022) of the Italian Ministry of University and Research (MUR), CUP: C53D23008370001 (Università degli Studi del Piemonte Orientale), E53D23017830001 (Politecnico di Torino), E53D23017840001 (Università degli Studi di Napoli), Consiglio Nazionale delle Ricerche (B53D23027682768).

Data Availability

Data will be made available on request.

References

[1] A.-G. Niculescu, A.M. Grumezescu, An up-to-date review of biomaterials application in wound management, Polymer (Basel) 14 (2022) 421.
[2] L. Su, Y. Jia, L. Fu, K. Guo, S. Xie, The emerging progress on wound dressings and their application in clinic wound management, Heliyon 9 (2023) e22520.
[3] D. Selvaraj, P. Viswanadha Vijaya, S. Elango, Wound dressings - a review, Biomed. (Taipei) 5 (2015) 22.
[4] A. Hiwrale, S. Bharati, P. Pingale, A. Rajput, Nanofibers: a current era in drug delivery system, Heliyon 9 (2023) e18917.
[5] A. Aluigi, A. Varesano, A. Montarsolo, C. Vineis, F. Ferrero, G. Mazzuchetti, C. Tonin, Electrospinning of keratin/poly(ethylene oxide)blend nanofibers, J. Appl. Polym. Sci. 104 (2007) 863–870.
[6] W. Ye, M. Qin, R. Qiu, J. Li, Keratin-based wound dressings: from waste to wealth, Int. J. Biol. Macromol. 211 (2022) 183–197.
[7] S. Quideau, D. Deffieux, C. Douat-Casassus, L. Pouységu, Plant polyphenols: chemical properties, biological activities, and synthesis, Angew. Chem. Int. Ed. Engl. 50 (2011) 586–621.
[8] E.-Q. Xia, G.-F. Deng, Y.-J. Guo, H.-B. Li, Biological activities of polyphenols from grapes, Int. J. Mol. Sci. 11 (2010) 622–646.
[9] A. Singh, P. Kaur, M. Kumar, S. Shafi, P.K. Upadhyay, A. Tiwari, V. Tiwari, N. K. Rangra, V. Thirunavukkarasu, S. Kumari, D. Roy, M. Ghosh, N. Arora, N. Sharma, Y. Garg, The role of phytochemicals in modulating the gut microbiota: Implications for health and disease, Med. Microecol. 24 (2025) 100125.
[10] W. Wu, Y. Mi, Q. Meng, N. Li, W. Li, P. Wang, Y. Hou, Natural polyphenols as novel interventions for aging and age-related diseases: Exploring efficacy, mechanisms of action and implications for future research, Chin. Herb. Med. 17 (2025) 279–291.
[11] S.T. Muntaha, A. Rakha, H. Rasheed, I. Fatima, M.S. Butt, G. Abdi, R.M. Aadil, Polyphenol-protein particles: a nutraceutical breakthrough in nutrition and food science, J. Agric. Food Res. 19 (2025) 101641.
[12] A. Shavandi, A.E.-D.A. Bekhit, P. Saeedi, Z. Izadifar, A.A. Bekhit, A. Khademhosseini, Polyphenol uses in biomaterials engineering, Biomaterials 167 (2018) 91–106.
[13] K. Schuhladen, J.A. Roether, A.R. Boccaccini, Bioactive glasses meet phytotherapeutics: The potential of natural herbal medicines to extend the functionality of bioactive glasses, Biomaterials 217 (2019) 119288.
[14] A.K. Das, K. Mitra, A.J. Conte, A. Sarker, A. Chowdhury, A.J. Ragauskas, Lignin - A green material for antibacterial application - A review, Int. J. Biol. Macromol. 261 (2024) 129753.
[15] M. Pourmadadi, Z. Omrani, R. Abbasi, M. Mirshafiei, F. Yazdian, Poly (Tannic Acid) based nanocomposite as a promising potential in biomedical applications, J. Drug. Deliv. Sci. Technol. 95 (2024) 105568.
[16] C. Chen, H. Yang, X. Yang, Q. Ma, Tannic acid: a crosslinker leading to versatile functional polymeric networks: a review, RSC Adv. 12 (2022) 7689–7711.
[17] B.K. Utpal, B. Sutradhar, M. Zehravi, S.H. Sweilam, U.P. Panigrahy, D. Urs, A. F. Fatima, P.K. Nallasivan, G.S. Chhabra, M. Sayeed, M.A. Alshehri, S.O. Rab, S. L. Khan, T.B. Emran, Polyphenols in wound healing: unlocking prospects with clinical applications, Naunyn. Schmiede Arch. Pharmacol. 398 (2025) 2459–2485.
[18] Z. Sun, X. Chen, X. Ma, X. Cui, Z. Yi, X. Li, Cellulose/keratin-catechin nanocomposite hydrogel for wound hemostasis, J. Mater. Chem. B Mater. Biol. Med. 6 (2018) 6133–6141.
[19] J. Zhang, X. Liu, Y. Sun, Z. Ge, J. Shen, J. Yuan, Quercetin@β-cyclodextrin conjugated keratin/polyurethane biocomposite mats for infected diabetic wound healing, Langmuir 40 (2024) 23673–23682.
[20] H. Jafari, P. Ghaffari-Bohlouli, M. Alishahi, F. Davani, S.S. Daneshi, R. Heidari, M. H. Morowvat, S.V. Niknezhad, L. Nie, H. Savoji, A. Shavandi, Tissue adhesive hydrogel based on upcycled proteins and plant polyphenols for enhanced wound healing, Mater. Today Chem. 33 (2023) 101722.

[21] M.R.V. Bertolo, S. Bogusz Junior, A.E. Mitchell, Green strategies for recovery of bioactive phenolic compounds from Agro-industrial wastes (pomegranate peels, almond hulls, and elderberry pomace) using natural deep eutectic solvents, ACS Food Sci. Technol. (2023).
[22] C. Jimenez-Lopez, M. Fraga-Corral, M. Carpena, P. García-Oliveira, J. Echave, A. G. Pereira, C. Lourenço-Lopes, M.A. Prieto, J. Simal-Gandara, Agriculture waste valorisation as a source of antioxidant phenolic compounds within a circular and sustainable bioeconomy, Food Funct. 11 (2020) 4853–4877.
[23] C. Wang, Y. You, W. Huang, J. Zhan, The high-value and sustainable utilization of grape pomace: A review, Food Chem. X 24 (2024) 101845.
[24] F. Marra, B. Petrovicova, F. Canino, A. Maffia, C. Mallamaci, A. Muscolo, Pomegranate wastes are rich in bioactive compounds with potential benefit on human health, Molecules 27 (2022) 5555.
[25] A. Aluigi, C. Tonetti, F. Rombaldoni, D. Puglia, E. Fortunati, I. Armentano, C. Santulli, L. Torre, J.M. Kenny, Keratins extracted from Merino wool and Brown Alpaca fibres as potential fillers for PLLA-based biocomposites, J. Mater. Sci. 49 (2014) 6257–6269.
[26] D.O. Sanchez Ramirez, C. Vineis, I. Cruz-Maya, C. Tonetti, V. Guarino, A. Varesano, Wool keratin nanofibers for bioinspired and sustainable use in biomedical field, J. Funct. Biomater. 14 (2022) 5.
[27] A. Varesano, A. Aluigi, C. Vineis, C. Tonin, Study on the shear viscosity behavior of keratin/PEO blends for nanofibre electrospinning, J. Polym. Sci. B Polym. Phys. 46 (2008) 1193–1201.
[28] S. Ferraris, M. Prato, C. Vineis, A. Varesano, G. Gautier di Confiengo, S. Spriano, Coupling of keratin with titanium: A physico-chemical characterization of functionalized or coated surfaces, Surf. Coat. Technol. 397 (2020) 126057.
[29] F. Heidenau, W. Mittelmeier, R. Detsch, M. Haenle, F. Stenzel, G. Ziegler, H. Gollwitzer, A novel antibacterial titania coating: metal ion toxicity and in vitro surface colonization, J. Mater. Sci. Mater. Med. 16 (2005) 883–888.
[30] G. Riccucci, M. Cazzola, S. Ferraris, V.A. Gobbo, M. Guaita, S. Spriano, Surface functionalization of Ti6Al4V with an extract of polyphenols from red grape pomace, Mater. Des. 206 (2021) 109776.
[31] G. Riccucci, S. Ferraris, C. Reggio, A. Bosso, G. Örlygsson, C.H. Ng, S. Spriano, Polyphenols from grape pomace: functionalization of chitosan-coated hydroxyapatite for modulated swelling and release of polyphenols, Langmuir 37 (2021) 14793–14804.
[32] S. Ferraris, X. Zhang, E. Prenesti, I. Corazzari, F. Turci, M. Tomatis, E. Vernè, Gallic acid grafting to a ferrimagnetic bioactive glass-ceramic, J. Non Cryst. Solids 432 (2016) 167–175.
[33] T.J. Herald, P. Gadgil, R. Perumal, S.R. Bean, J.D. Wilson, High-throughput micro-plate HCI-vanillin assay for screening tannin content in sorghum grain: High-throughput HCl-vanillin assay for screening tannin in sorghum, J. Sci. Food Agric. 94 (2014) 2133–2136.
[34] M.L. Alfieri, G. Pilotta, L. Panzella, L. Cipolla, A. Napolitano, Gelatin-based hydrogels for the controlled release of 5,6-dihydroxyindole-2-carboxylic acid, a melanin-related metabolite with potent antioxidant activity, Antioxid. (Basel) 9 (2020) 245.
[35] M.L. Alfieri, G. Riccucci, S. Ferraris, A. Cochis, A.C. Scalia, L. Rimondini, L. Panzella, S. Spriano, A. Napolitano, Deposition of antioxidant and cytocompatible caffeic acid-based thin films onto Ti6Al4V alloys through hexamethylenediamine-mediated crosslinking, ACS Appl. Mater. Interfaces 15 (2023) 29618–29635.
[36] R. Apak, K. Güçlü, M. Ozyürek, S.E. Karademir, Novel total antioxidant capacity index for dietary polyphenols and vitamins C and E, using their cupric ion reducing capability in the presence of neocuproine: CUPRAC method, J. Agric. Food Chem. 52 (2004) 7970–7981.
[37] S.L. Alfonso García, M.T. Parada-Sanchez, D. Arboleda Toro, The phenotype of gingival fibroblasts and their potential use in advanced therapies, Eur. J. Cell. Biol. 99 (2020) 151123.
[38] A. Fadl, A. Leask, Hiding in plain sight: human gingival fibroblasts as an essential, yet overlooked, tool in regenerative medicine, Cells 12 (2023) 2021.
[39] M. Bergoglio, M. Kriehuber, B. Sölle, E. Rossegger, S. Schlögl, Z. Najmi, A. Cochis, F. Ferla, M. Miola, E. Vernè, M. Sangermano, 3D-printed acrylated soybean oil scaffolds with vitrimeric properties reinforced by Tellurium-doped bioactive glass, Polym. (Basel) 16 (2024) 3614.
[40] F. Gamna, S. Yamaguchi, A. Cochis, S. Ferraris, A. Kumar, L. Rimondini, S. Spriano, Conferring antioxidant activity to an antibacterial and bioactive titanium surface through the grafting of a natural extract, Nanomater. (Basel) 13 (2023) 479.
[41] M. Jackson, H.H. Mantsch, The use and misuse of FTIR spectroscopy in the determination of protein structure, Crit. Rev. Biochem. Mol. Biol. 30 (1995) 95–120.
[42] M. Di Foggia, C. Boga, G. Micheletti, B. Nocentini, P. Taddei, Vibrational Raman and IR data on brown hair subjected to bleaching, Data Brief. 38 (2021) 107439.
[43] P. Erra, N. Gómez, L.M. Dolcet, M.R. Juliá, D.M. Lewis, J.H. Willoughby, FTIR analysis to study chemical changes in wool following a sulfitolysis treatment, Text. Res. J. 67 (1997) 397–401.
[44] A. Varesano, C. Vineis, C. Tonetti, D.O.S. Ramírez, G. Mazzuchetti, Chemical and physical modifications of electrospun keratin nanofibers induced by heating treatments, J. Appl. Polym. Sci. 131 (2014).
[45] F. Moccia, A.C. Flores-Gallegos, M.L. Chávez-González, L. Sepúlveda, S. Marzorati, L. Verotta, L. Panzella, J.A. Ascacio-Valdes, C.N. Aguilar, A. Napolitano, Ellagic acid recovery by solid state fermentation of pomegranate wastes by Aspergillus niger and Saccharomyces cerevisiae: a comparison, Molecules 24 (2019) E3689.
[46] F. Moccia, S. Agustin-Salazar, L. Verotta, E. Caneva, S. Giovando, G. D'Errico, L. Panzella, M. d'Ischia, A. Napolitano, Antioxidant properties of agri-food byproducts |and specific boosting effects of hydrolytic treatments, Antioxid. (Basel) 9 (2020) E438.
[47] L. Panzella, F. Moccia, R. Nasti, S. Marzorati, L. Verotta, A. Napolitano, Bioactive phenolic compounds from agri-food wastes: An update on green and sustainable extraction methodologies, Front. Nutr. 7 (2020) 60.
[48] G. Mugnaini, M. Bonini, L. Gentile, O. Panza, M.A. Del Nobile, A. Conte, R. Esposito, G. D'Errico, F. Moccia, L. Panzella, Effect of design and molecular interactions on the food preserving properties of alginate/pullulan edible films loaded with grape pomace extract, J. Food Eng. 361 (2024) (Not Available).
[49] S. Ferraris, F. Truffa Giachet, M. Miola, E. Bertone, A. Varesano, C. Vineis, A. Cochis, R. Sorrentino, L. Rimondini, S. Spriano, Nanogrooves and keratin nanofibers on titanium surfaces aimed at driving gingival fibroblasts alignment and proliferation without increasing bacterial adhesion, Mater. Sci. Eng. C. Mater. Biol. Appl. 76 (2017) 1–12.
[50] S. Ferraris, S. Spriano, A.C. Scalia, A. Cochis, L. Rimondini, I. Cruz-Maya, V. Guarino, A. Varesano, C. Vineis, Topographical and biomechanical guidance of electrospun fibers for biomedical applications, Polym. (Basel) 12 (2020) 2896.
[51] F. Daou, C. Reggio, M. Manfredi, H. Abreu, G. Cappellano, M. Nascimben, G. Örlygsson, C.H. Ng, A. Bosso, S. Ferraris, S. Spriano, A. Cochis, Polyphenols promote stem cell surface adaptation onto low-adhesion chitosan-titanium through protein synthesis and cytoskeletal remodeling, Biomater. Adv. 180 (2026) 214584.
[52] M. Miłek, D. Marcinčáková, J. Legáth, Polyphenols content, antioxidant activity, and cytotoxicity assessment of Taraxacum officinale extracts prepared through the Micelle-mediated extraction method, Molecules 24 (2019) E1025.
[53] D. Pattarayan, A. Sivanantham, R. Bethunaickan, R. Palanichamy, S. Rajasekaran, Tannic acid modulates fibroblast proliferation and differentiation in response to pro-fibrotic stimuli, J. Cell. Biochem. 119 (2018) 6732–6742.
[54] A.L. Boehning, S.A. Essien, E.L. Underwood, P.K. Dash, D. Boehning, Cell type-dependent effects of ellagic acid on cellular metabolism, Biomed. Pharmacother. 106 (2018) 411–418.
[55] S.U. Mertens-Talcott, S.T. Talcott, S.S. Percival, Low concentrations of quercetin and ellagic acid synergistically influence proliferation, cytotoxicity and apoptosis in MOLT-4 human leukemia cells, J. Nutr. 133 (2003) 2669–2674.
[56] R. Guarnieri, R. Reda, D. Di Nardo, G. Miccoli, A. Zanza, L. Testarelli, vitro direct and indirect cytotoxicity comparative analysis of one pre-hydrated versus one dried acellular porcine dermal matrix, Mater. (Basel) 15 (2022) 1937.
[57] A.-M. Brezoiu, C. Matei, M. Deaconu, A.-M. Stanciuc, A. Trifan, A. Gaspar-Pintiliescu, D. Berger, Polyphenols extract from grape pomace. Characterization and valorisation through encapsulation into mesoporous silica-type matrices, Food Chem. Toxicol. 133 (2019) 110787.
[58] M.F. Motta, A.F. Vattimo, F. Amone, R. Malivindi, O.I. Parisi, F. Puoci, Valorization of grape pomace extract through dextran–grape conjugates: A sustainable approach for cosmetic and dermatological applications, Appl. Sci. (Basel) 15 (2025) 3220.
[59] M.H. Hashemi Poor, S. Hosseinzadeh, M. Aminlari, Wound healing potential of pomegranate peel extract in human dermal fibroblasts through regulating the expression of FN1 gene, S. Afr. J. Bot. 146 (2022) 222–229.
[60] J. Du, H. Wang, L. Zhong, S. Wei, X. Min, H. Deng, X. Zhang, M. Zhong, Y. Huang, Bioactivity and biomedical applications of pomegranate peel extract: a comprehensive review, Front. Pharmacol. 16 (2025) 1569141.
[61] J. da, C. Lopes, J. Madureira, F.M.A. Margaça, S. Cabo Verde, Grape pomace: A review of its bioactive phenolic compounds, health benefits, and applications, Molecules 30 (2025) 362.
[62] M. Jalouli, M.A. Rahman, P. Biswas, H. Rahman, A.H. Harrath, I.-S. Lee, S. Kang, J. Choi, M.N. Park, B. Kim, Targeting natural antioxidant polyphenols to protect neuroinflammation and neurodegenerative diseases: a comprehensive review, Front. Pharmacol. 16 (2025) 1492517.
[63] R.F. Abutayeh, M.A.K. Ayyash, R.A. Alwany, A. Abuodeh, K. Jaber, M.A.A. Al-Najjar, Exploring the antimicrobial potential of pomegranate peel extracts (PPEs): Extraction techniques and bacterial susceptibility, PLoS. One 19 (2024) e0315173.
[64] D. Sateriale, G. Forgione, M. Di Rosario, C. Pagliuca, R. Colicchio, P. Salvatore, M. Paolucci, C. Pagliarulo, Vine-winery byproducts as precious resource of natural antimicrobials: In vitro antibacterial and antibiofilm activity of grape pomace extracts against foodborne pathogens, Microorganisms 12 (2024) 437.
[65] A. Salim, L. Marquez, K. Jakkala, S. Woo, M. Caputo, F. Fancello, P. Deiana, M. Santona, M.G. Molinu, C.L. Quave, S. Zara, Identification of punicalagin as a key bioactive compound responsible for the antimicrobial properties of Punica granatum L. peel extract against Staphylococcus aureus, J. Agric. Food Chem. 73 (2025) 18280–18290.
[66] O. Panza, M.L. Alfieri, M.A. Del Nobile, G. Mugnaini, A. Conte, L. Panzella, M. Bonini, Effects of dehydration temperature on physico-chemical, antioxidant and antimicrobial properties of grape pomace powder, Leb. Wiss. Technol. 227 (2025) 118029.